C.P. No. 1262




**MINISTRY OF DEFENCE (PROCUREMENT EXECUTIVE)**

*AERONAUTICAL RESEARCH COUNCIL*

*CURRENT PAPERS*

# Aerodynamic Characteristics of NPL 9626 and NPL 9627, Further Aerofoils Designed for Helicopter Rotor Use

*By*

*P. G. Wilby, N. Gregory and V. G. Quincey,*

*Aerodynamics Division, NPL*

LONDON· HER MAJESTY'S STATIONERY OFFICE

1973

PRICE 60p NET

CP No. 1262*
November, 1969

# AERODYNAMIC CHARACTERISTICS OF NPL 9626 AND NPL 9627, FURTHER AEROFOILS DESIGNED FOR HELICOPTER ROTOR USE

- by -
P. G. Wilby, N. Gregory and V. G. Quincey,
Aerodynamics Division, NPL

## SUMMARY

Aerodynamic characteristics and ordinates are given for two modifications to the NACA 0012 profile with leading-edge camber that have been designed to produce reductions in wave drag in transonic flow. Analyses of hovering helicopter performance are given, to indicate the improvements that would follow from the adoption of either of these new aerofoils.

## 1. Introduction

Earlier work[1] led to the design of the NPL 9620 profile, a modification to NACA 0012, which had a thicker, slightly drooped nose, and was designed in an attempt to weaken slightly the upper-surface shock wave at Mach numbers between 0.55 and 0.75 and so to reduce profile drag in conditions where the wave-drag contribution is significant. The aim was to improve the performance of the Sud Aviation SA330E helicopter in hover in high-altitude conditions, since it was thought that the rotor was experiencing local regions of supersonic flow and shock waves near the blade tip and hence high values of the drag coefficient in these conditions.

One of the constraints applied to the design of the NPL 9620 aerofoil, was that in order to be applicable to the SA 330E rotor without extensive re-design and re-validation of the rotor, the modification could not extend forward beyond the original nose of NACA 0012 profile and the section between 3% and 30% of the chord had to be no thinner than the original profile in order not to reduce the wall thickness and the strength of the hollow spar.

The section NPL 9620 was found, experimentally, to possess some slight advantages over NACA 0012, but the pressure distribution turned out not to be of the desired "peaky" type at the high values at $C_L$ which were of interest. Further profiles were therefore designed with the object of obtaining a "peaky" type pressure distribution thereby further weakening the shock-wave and giving still more improvements in performance.

The/

*Replaces A.R.C.31 687 - NPL Aero Special Report 036.

The present paper reports on the characteristics of two new aerofoils that show appreciable performance improvements relative to both NACA 0012 and NPL 9620. Wind tunnel test conditions are described in §2 and the profile ordinates and a discussion of the measured aerodynamic characteristics of the sections are given in §3. In §4 an analysis is given of the hover requirements of Westland Wessex and Sud 330 helicopters using results obtained by the theoretical calculation method recently developed at Westland Helicopters Ltd[2]. The changes in drag distribution along the span of the blade that would stem from the adoption of each profile are indicated and an estimate is made of the profile power saving.

## 2. Test Conditions

Wind-tunnel tests on these aerofoils were carried out in the NPL 36 in × 14 in (0.92 m × 0.36 m) transonic tunnel under the same conditions that were used for tests on previous aerofoil profiles intended for use on helicopter rotor blades[1,4]. The models were of 0.254 m (10 in) chord and spanned the 0.36 m (14 in) dimension of the tunnel, which operates at atmospheric stagnation pressure, giving Reynolds numbers that vary from about $1.7 \times 10^6$ at $M = 0.3$ to about $3.6 \times 10^6$ at $M = 0.8$. The floor and ceiling of the tunnel were slotted (4 slots, overall open-area ratio = 0.033) and were 0.79 m (31 in) apart throughout the length of the working section: these conditions are close to those that give blockage-free results. No corrections have been applied for lift interference. Values of $C_{Lmax}$ at lower Mach numbers are known to be depressed on account of the departure from two-dimensional conditions initiated by premature separation of the thick end-wall boundary-layer, but this is not thought to affect the comparative assessment of the performance of aerofoils that are essentially of the same family.

All measurements were obtained with a roughness band of 230-270 mesh carborundum* present between 0 and 2% chord on both surfaces. Sufficient roughness was required to produce boundary-layer transition ahead of strong shocks in order to avoid optimistic values of $C_{Lmax}$ at high Mach number. On the other hand, too much roughness was likely to produce low values of $C_{Lmax}$ at lower speeds and a high overall level of drag. The band was chosen, as a result of investigations briefly described in Reference 3, to provide a reasonable compromise roughness that could be used over the whole test range and was the same on both models and the same as used in previous tests[1,4]. An indication that comparable conditions existed on the two aerofoils was given by the fact that the pressure ahead of the shock-wave at shock-induced separation was the same for each aerofoil.

Lift and pitching moments were found by integration of pressure measured at static-pressure holes in the surface of the model, and profile drag was obtained by wake travers.

3./

---

* 230-270 mesh carborundum implies grains that were sifted through a gauze with 230 wires to the inch, but which were retained by a gauze with 270 wires to the inch. This implies grains that passed through a square aperture of side 0.062 mm (0.0027 in) but not through one with side (0.053 mm) 0.0023 in.

## 3. Aerodynamic Characteristics of the Two New Aerofoils

NPL 9626 is a development of NPL 9620 in that its profile differs only over the forward 30% of the upper surface. This profile change enabled the desired form of peaky pressure distribution to be attained at Mach numbers between 0.6 and 0.7. Thus, in this Mach number range NPL 9626 generates a weaker shock-wave, for a given $C_L$, than either NPL 9620 or NACA 0012, resulting in a higher $C_{Lmax}$ and a lower wave drag. In Figs.1 and 2 the values of $C_{Lmax}$ and drag coefficient for the new section are compared, over the full Mach number range, with those for NACA 0012 and NPL 9615 (a section based on NACA 0012 but incorporating leading-edge extension as well as droop - see Reference 4). The main points to note are that the $C_{Lmax}$ of NPL 9626 at Mach numbers between 0.6 and 0.7 is equal to that for NPL 9615 and the supercritical drag over this range is actually less than for NPL 9615. In this region NPL 9626 has a considerably better performance than NACA 0012 and is also superior to NPL 9620. However, there appears to be a penalty at Mach numbers around 0.5, where NPL 9626 has the highest supercritical drag.

A further aerofoil, NPL 9627, was designed in an attempt to overcome the disadvantages of NPL 9626 at M = 0.5, and at the same time the lower surface was modified to make the aerofoil thickness compatible with the Sud spar, with the proviso that the spar is tilted even further down than would be necessary for NPL 9620[1]. It will be realized that the modifications that lead to NPL 9626 resulted in a aerofoil section that can not be incorporated in the Sud blade without leaving unacceptably thin spar walls. The profiles are compared in Fig.3 and their ordinates given in Table 1.

It is seen in Figs.4 and 5, which give $C_{Lmax}$ boundary and drag polars for NPL 9627, that this latest aerofoil does in fact have an improved performance over both NPL 9626 and NACA 0012 at M = 0.5, and for M<0.4 its lifting ability is comparable with that of NPL 9615. However, NPL 9627 is not as good as NPL 9626 for M>0.55, although it is still an improvement on NACA 0012 and NPL 9620. The variation of $C_L$ with Mach number and incidence is shown in Figs.6 and 7 for both these new aerofoils.

The variations of $C_D$ with $C_L$ for both NPL 9626 and NPL 9627 are directly compared in Figs.8 to 11 for various Mach numbers in the important range of 0.5 to 0.65. Also in these figures are included results for NACA 0012, NPL 9615 and NPL 9620, but the important comparison for present purposes is between the two new aerofoils and NACA 0012. This comparison shows that NPL 9626 has the best performance at the higher Mach numbers but this advantage is off set by its inferior performance at M = 0.5. Though not as good as 9626 at the higher M, 9627 is superior to NACA 0012 in all supercritical conditions.

Having seen how the aerofoils perform relatively to one another it is of interest to examine some of their typical pressure distributions so as to gain an insight into their different behaviour. Pressure distributions are shown in Fig.12 for NACA 0012, NPL 9626 and NPL 9627 at M = 0.65 and an incidence of 6°. The peaky nature of the NPL 9626 pressure distribution is immediately noticed and is seen to lead to a much weaker shock-wave than is found on either of the other aerofoils and hence a much lower value of drag. On NPL 9627 the local flow velocity on the upper surface is seen to increase between 10 and 20% chord, resulting in what may be an unnecessarily strong shock-wave. This is still, however, weaker than that found on NACA 0012. A similar situation is found at the lower Mach number of 0.6 where NPL 9627 maintains its advantage over NACA 0012 by virtue of the lower velocities in the region ahead of the shock-wave.

This/

This results in a weaker shock for a given $C_L$ or, as is shown in Fig.13, a similar shock strength for a considerably higher value of $C_L$. The peaky nature of NPL 9626 allows it to sustain high velocities near the leading edge and yet have a shock strength comparable with that on NPL 9627. The lower drag of NPL 9626 may be due to the extra suction effect on the forward-facing surface, near the leading-edge, that results from the high velocities there. It is however these high velocities near the leading-edge that contribute to the inferior performance of NPL 9626 at M = 0.5 when the leading-edge peak is followed immediately by a recompression to subsonic conditions (see Fig.14). With this recompression so close to the leading-edge there is no chance for an isentropic recompression to take place ahead of the shock-wave, leaving NPL 9626 with the strongest shock-wave and the worst performance. NPL 9627, on the other hand, was designed specifically to reduce the velocity peak at M = 0.5 and this has led to its superior performance at this Mach number. The complete variation of peak height with $C_L$ for these aerofoils at a Mach number 0.5 is shown in Fig.15.

The reduction of velocity over the first 3% chord, that was designed for in NPL 9627, has achieved the desired effect of improving the performance of this section relative to that of NACA 0012 and NPL 9626 at M = 0.5. However, velocity increases have appeared between 10 and 20% chord which have prevented the peaky type of pressure distribution, found on NPL 9626, from developing at higher Mach numbers. Thus the gains at these Mach numbers are not as great as for NPL 9626.

Apart from the variation of drag coefficient with lift coefficient at constant Mach number, the variation of drag coefficient with Mach number at constant incidence is also of interest. Such variations are compared in Fig.16 for NACA 0012 and NPL 9626 for the values of incidence at which the characteristics of the two aerofoils differ most. The very rapid rise of drag does not immediately follow the attainment of critical conditions but is separated by an intermediate region of supercritical drag-creep. The rate and extent of this drag-creep varies according to the way in which the supercritical flow develops; and for NPL 9626 this is such as to delay the rapid drag-rise to a higher value of Mach number than for NACA 0012. This delay is particularly pronounced at incidences between 4° and 7°. Fig.17 compares the variations of drag coefficient with Mach number for NPL 9626 and NPL 9627 and it is seen that although the rapid drag-rise has not been delayed on NPL 9627 to quite the same extent as on NPL 9626, the former has a much less pronounced drag-creep in the Mach number range 0.45 to 0.575. The reasons for these differences can of course be traced to the different shock strengths that are responsible for the variations in $C_{Lmax}$ that have already been discussed.

So far no mention has been made of that very important quantity pitching moment, but the variation of quarter-chord pitching moment with incidence and Mach number is shown in Figs.18 and 19 for NPL 9626 and NPL 9627 respectively. A comparison of these figures with the results for NACA 0012 (Ref.1 and 4) shows that the overall pattern of the pitching moment variation is rather similar for all three aerofoils although there is of course a progressive distortion of the individual curves, in the sense of a general downward displacement, with increasing camber. Also, the fact that the new aerofoils continue to produce lift after NACA 0012 has stalled, means that the peaks in the pitching moment curves, which are associated with the stall, have an additional displacement. The nose-down pitching-moment increment that is associated with camber is illustrated in Fig.20 where the variation of quarter-chord pitching moment coefficient with Mach number is shown for zero incidence. The curve for NPL 9615 is also included as an extra datum and it is seen that the curves for NPL 9626 and 9627 are very similar in shape to that for NPL 9615 but the sudden increase of pitching moment occurs at an earlier stage

for/

for the new aerofoils. The fact that the accelerated decrease of pitching moment is halted earlier means that the magnitude of the variation of pitching moment is less than for NPL 9615. This sudden change from decreasing to increasing pitching moment is due, not to boundary-layer separation, but to the appearance and development of supersonic flow on the lower surface of the aerofoil.

## 4. Analysis of Hover Requirements on Rotors

Consideration of all the variables involved shows that the performance of a given hovering rotor is governed by the following dimensionless parameters,

$$C_T/S \qquad (\equiv W/nc\rho_o\sigma R^3\Omega^2)$$

and $$M_{tip} \qquad (\equiv \Omega R/a),$$

the geometrical variables $\theta_o$, A, B, and $\gamma$ (collective and cyclic pitches and shaft-tilt) being adjusted to give the desired thrust W and to trim both rotor and helicopter. The relative air density ($\sigma$) and the speed of sound (a) vary with temperature and altitude and are conveniently defined by the height and the difference in temperature $\Delta t$ between the actual temperature and the standard atmosphere (ISA) temperature for the given height. $C_T$, the rotor thrust coefficient, represents the thrust non-dimensionalised in terms of disc area and tip velocity, and for a given rotor (i.e., given solidity (s), twist, chord (c) and profile distribution) $C_T/S$ completely determines the radial distribution of blade section lift coefficient, $C_L$.

Calculations of blade loading have been carried out by C. V. Cook of Westland Helicopters Ltd, using their latest computer programme, which takes slipstream contraction into account[2], and the results from a typical computation for a Wessex blade with NACA 0012 section are shown as curve (a) in Fig.21 where the local blade incidence is shown as a function of Mach number, together with the incidence boundaries for maximum lift and drag rise. At a somewhat higher all-up-weight, altitude and rotational speed, the effect of further increase in height is shown by the comparison between curves (b) and (c). In both these later cases the tip of the blade is in drag-rise conditions, in the second case significantly so, as is shown by the radial distribution of blade drag coefficient (Fig.22).

The movement of the incidence peak to higher Mach numbers (Fig.21) is more serious than the increase in peak incidence itself so it is instructive to consider an incidence peak at 6° and M = 0.6 and to consider approximately how this would be shifted by alterations to relevant parameters (Fig.23).

A given percentage change in all-up-weight would result in a similar change in incidence without alteration to tip Mach number.

An increase in altitude at a given all-up-weight say +2400 m, reduces the temperature and hence increases the Mach number as well as increasing $C_L$ and incidence to compensate for the density change. This is a worse type of change than the previous one.

A temperature change alone affects both Mach number and density, and results in a movement parallel to the drag-rise boundary of NACA 0012.

A/

A change in rotational speed, although it effects a big change in Mach number, would not, unless accompanied by rotor design changes, prevent the tip of the blade encountering drag-rise conditions since the movement of the incidence peak is again roughly parallel to the drag-rise boundary.

It is thus seen that it is difficult to make an appreciable improvement on the hover performance of a helicopter by changing the various parameters that govern the motion of the blade. The other possibilities are alterations to the blade geometry. An increase in the number or chord of the blades would reduce the $C_L$ required but would not necessarily effect any reduction in power; the change that would yield a direct performance improvement is a change of blade section to the type that produces a movement of the drag-rise boundary. Fig.24 compares the drag-rise boundaries, and also the $C_{Lmax}$ boundaries, for the two new aerofoils described in this report with the boundaries for NACA 0012 and NPL 9615. Also in the figure is shown the most severe of the operating conditions for the Wessex helicopter in hover, as presented in Fig.21. The change of the drag-rise boundary produced by the new sections is such as would relieve the high drag problem encountered by the blade tip, as not only is there a sideways displacement of the boundary as a whole but there is also a bulge that appears in the boundary in precisely the region in which the tip operates. It should be pointed out that, at incidences of 5° and above, the drag rise becomes less well-defined than at lower incidences (see Figs.16 and 17) and the boundaries drawn in Fig.24 mark the onset of the very rapid rise of drag that follows the initial drag-creep.

The radial distributions of drag coefficient that would result from the use of the various sections on the Wessex rotor under the most severe of the hover conditions is shown in Fig.25. As torque due to profile drag is proportional to $C_D \left(\frac{r}{R}\right)^3$, it is reductions of drag at the tip that are most significant and it is here that the major drag reductions would result from the use of the new sections. A change of aerofoil from NACA 0012 to NPL 9615 or NPL 9626 yields a reduction of profile power of 16% and a change to NPL 9627 yields a 13% reduction. Near the tip of this rotor, where the Mach number exceeds 0.6, NPL 9626 has a lower drag than NPL 9615 but the situation is reversed at stations slightly further inboard where the Mach number is in the range 0.5 to 0.575. This explains why the profile power would be the same for each of these sections in spite of their different characteristics.

The SUD 330E helicopter has an almost identical tip speed of 208 m/s at 44.2 rev/s and therefore yields similar results. Four cases have been evaluated as indicated by the Table below, and the blade incidence demands are shown in Fig.26. The first three cases are at nominally the same all-up-weight and various altitude and temperature conditions. The fourth case 'd', at slightly lighter weight (and not maximum $W/\sigma$), is at very high altitude in cold conditions, and these two features combine to produce a much higher tip Mach number; in these conditions the rotor is seriously in drag-rise difficulties, Fig.27 (Case 'd'). At the lower tip Mach numbers, although, only the extreme tip of the blade is in drag rise, as is shown by Case 'c' in Fig.27, the incursion is such that a reduction of approximately 10% in profile power can be

Table

SUD 330 helicopter hover cases

| Case | Weight | W/ | Altitude | Temperature Condition |
|---|---|---|---|---|
| a | 6550 kg | 6550 kg | 0 m | ISA |
| b | 6520 kg | 7150 kg | 1160 m | ISA-6° |
| c | 6480 kg | 8070 kg | 1525 m | ISA+20° |
| d | 6160 kg | 7720 kg | 3350 m | ISA-20° |

achieved/

achieved by changing the rotor blade profile to NPL 9615. Both the present sections exhibit the slightly smaller saving of 8% in power, the poor performance of NPL 9626 at $r/R = 0.95$ and a Mach number of 0.575 being particularly noticeable.

In case 'd', when the tip Mach number is higher, the use of NPL 9626 would produce more pronounced improvements, particularly as the inboard region when the Mach number is just below 0.575 is at a low enough incidence not to provoke drag-creep problems. The resulting reduction in power in this hover case could be as high as 21% with NPL 9626, compared with 16% for NPL 9627, but the region of poor performance of NPL 9626 would be entered by the rotor tip at 0° azimuth in highly loaded, high forward-speed conditions. Hence, in spite of its less dramatic advantages in the hover condition, the NPL 9627 section, whose aerodynamic characteristics are everywhere better than those of NACA 0012, should be regarded as the better section for all-round helicopter rotor use.

## 5. Conclusions

Two further cambered modifications to the front of NACA 0012 profile are described. The first, NPL 9626, successfully generates much lower wave drag at a given $C_L$ at Mach numbers between 0.6 and 0.7 with high $C_L$ max both in this range and at low Mach numbers. At Mach numbers between 0.5 and 0.575 the performance is poor, both for $C_{Lmax}$ and for profile drag: in some conditions the drag is greater than on NACA 0012.

The second profile, NPL 9627, was designed specifically for a reduced velocity peak at Mach numbers around 0.5, and has a lower-surface shape adjusted to maintain the local profile thickness of NACA 0012 and therefore to suit the SUD 330 main spar (in a tilted position). This aerofoil shows improvements over both NACA 0012 and the earlier NPL 9620 at Mach numbers greater than 0.55 though it is not so good as NPL 9626. It remains better than NACA 0012 and is considerably better than NPL 9626 at a Mach number of 0.5. At low Mach number its lifting ability matches that of all the earlier cambered modifications.

Based on the measured steady-flow aerodynamic characteristics, the effectiveness of these aerofoils in reducing profile power on a hovering rotor in limiting conditions has been examined theoretically for both Wessex and SUD 330 rotors. In conditions where drag rise occurs, NPL 9615 and NPL 9627 have shown savings of between 8% and 16% in profile power over NACA 0012; the saving increases with tip Mach number. NPL 9626, though similar to NPL 9627 at low tip Mach numbers becomes progressively better as tip Mach number increases, yielding over 20% improvement in a particular case. However, the region of poor performance in the limited Mach number range 0.5 - 0.575 could be encountered by the blade in certain sectors at high forward speed, so that NPL 9627 is to be preferred for all-round use.

## Acknowledgements

Acknowledgement is due to Mr. M. Ralph and to Mr. K. Bartlett for their assistance with the experimental work in the 36 in × 14 in wind tunnel. Acknowledgement is also due to Sud Aviation and Westland Helicopters Ltd, for data supplied, and particularly to Mr. C. V. Cook of the latter firm for managing the performance calculations on his firm's computer.

---

References/

## References


| No. | Author(s) | Title, etc. |
|---|---|---|
| 1 | N. Gregory and P. G. Wilby | Wind-tunnel tests of NPL 9620 - a derivative of NACA 0012 with decreased supercritical drag for helicopter rotor use. Unpublished NPL results. |
| 2 | C. V. Cook | Rotor performance prediction in hover. A.R.C.30 845 - P.L.517. Westland Helicopters Ltd., Research Paper 357. November, 1968. |
| 3 | P. G. Wilby and V. G. Quincey | Some effects due to different carborundum bands on the leading-edges of aerofoils at high incidence in a subsonic free-stream. NPL Aero Note 1081. July, 1969. |
| 4 | N. Gregory and P. G. Wilby | NPL 9615 and NACA 0012 - A comparison of aerodynamic data. NPL Aero Special Report 017. A.R.C.30 657 - Perf.2755 - P.L.504. 5th November, 1968. |


---

TABLE 1/

**TABLE 1**

NPL 9626 and NPL 9627 Ordinates

| NPL 9626 | | | NPL 9627 | |
|---|---|---|---|---|
| X/C | (y/c)u | (y/c)ℓ | (y/c)u | (y/c)ℓ |
| 0 | - 0.01100 | - 0.01100 | - 0.01600 | - 0.01600 |
| 0.00020 | - 0.00791 | - 0.01342 | - 0.01301 | - 0.01842 |
| 0.00050 | - 0.00613 | - 0.01482 | - 0.01127 | - 0.01982 |
| 0.00100 | - 0.00415 | - 0.01637 | - 0.00935 | - 0.02137 |
| 0.00160 | - 0.00238 | - 0.01772 | - 0.00764 | - 0.02272 |
| 0.00241 | - 0.00054 | - 0.01912 | - 0.00583 | - 0.02412 |
| 0.00350 | + 0.00159 | - 0.02047 | - 0.00389 | - 0.02547 |
| 0.00500 | 0.00356 | - 0.02192 | - 0.00132 | - 0.02692 |
| 0.00650 | 0.00522 | - 0.02337 | + 0.00060 | - 0.02837 |
| 0.00800 | 0.00667 | - 0.02457 | 0.00243 | - 0.02957 |
| 0.00961 | 0.00816 | - 0.02557 | 0.00415 | - 0.03057 |
| 0.01500 | 0.01202 | - 0.02878 | 0.00896 | - 0.03378 |
| 0.02153 | 0.01574 | - 0.03155 | 0.01336 | - 0.03655 |
| 0.03806 | 0.02237 | - 0.03703 | 0.02183 | - 0.04203 |
| 0.05904 | 0.02919 | - 0.04199 | 0.02872 | - 0.04762 |
| 0.08427 | 0.03572 | - 0.04670 | 0.03548 | - 0.05279 |
| 0.11349 | 0.04202 | - 0.05106 | 0.04182 | - 0.05707 |
| 0.14645 | 0.04775 | - 0.05494 | 0.04725 | - 0.06035 |
| 0.18280 | 0.05267 | - 0.05787 | 0.05173 | - 0.06261 |
| 0.22221 | 0.05644 | - 0.05979 | 0.05502 | - 0.06382 |
| 0.26430 | 0.05891 | - 0.06074 | 0.05730 | - 0.07399 |
| 0.30866 | 0.05999 | - 0.06067 | 0.05849 | - 0.06313 |
| 0.35486 | 0.05938 | - 0.05971 | 0.05866 | - 0.06134 |
| 0.40245 | 0.05794 | - 0.05794 | 0.05764 | - 0.05875 |
| 0.45099 | 0.05576 | - 0.05576 | 0.05574 | - 0.05600 |
| 0.5 | 0.05294 | - 0.05294 | 0.05294 | - 0.05294 |
| 0.54901 | 0.04960 | | | |
| 0.59755 | 0.04583 | | | |
| 0.64514 | 0.04176 | | | |
| 0.69134 | 0.03747 | SYMMETRIC REAR | | |
| 0.73570 | 0.03308 | HALF IDENTICAL | | |
| 0.77779 | 0.02866 | TO NACA 0012 | | |
| 0.81720 | 0.02430 | | | |
| 0.85355 | 0.02011 | | | |
| 0.88651 | 0.01614 | | | |
| 0.91573 | 0.01250 | | | |
| 0.94096 | 0.00925 | | | |
| 0.96194 | 0.00648 | | | |
| 0.97847 | 0.00424 | | | |
| 0.99039 | 0.00260 | | | |
| 0.99759 | 0.00160 | | | |
| 1.0 | 0.00126 | | | |

JED

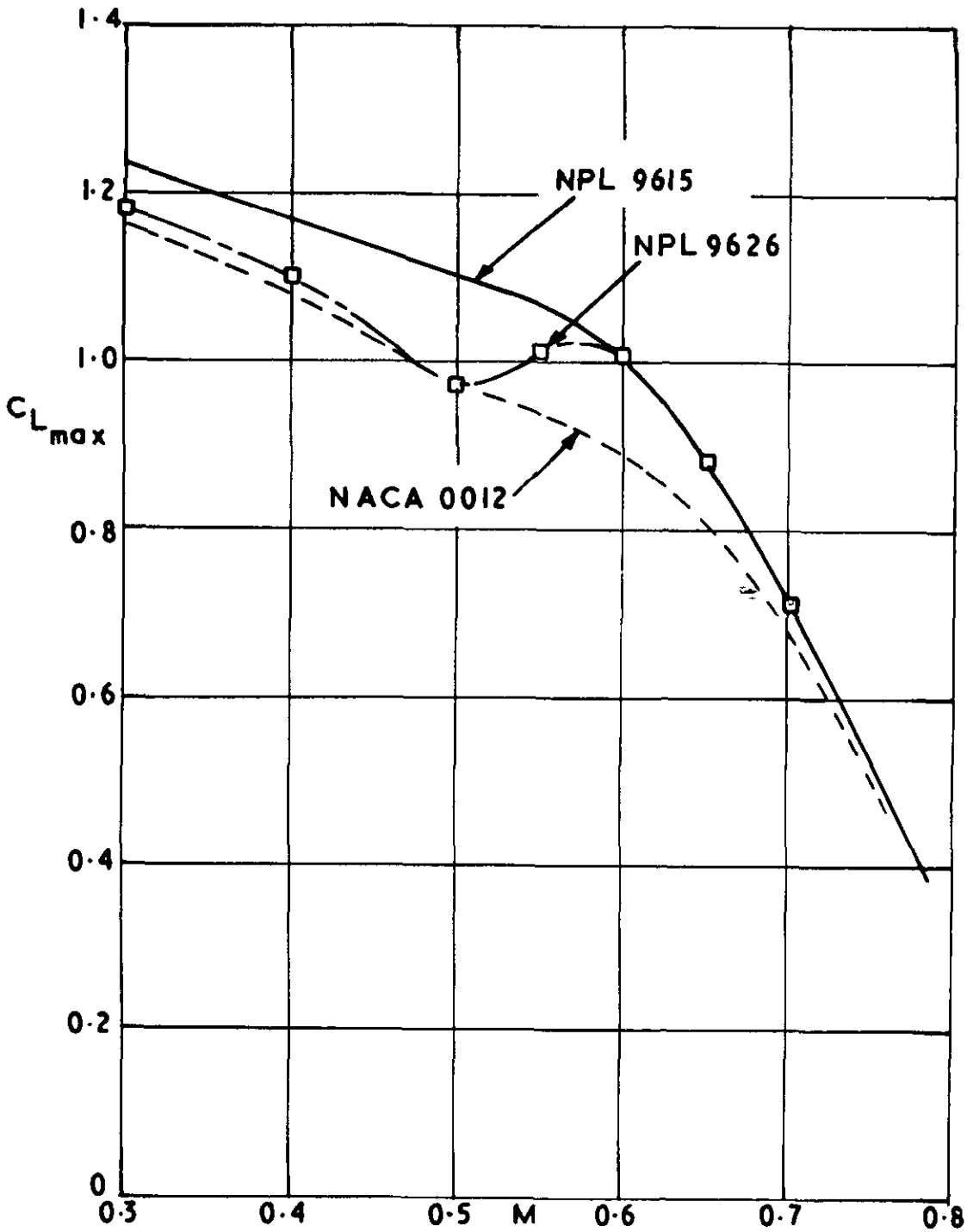


Variation of $C_{L_{max}}$ with Mach number for NPL 9626

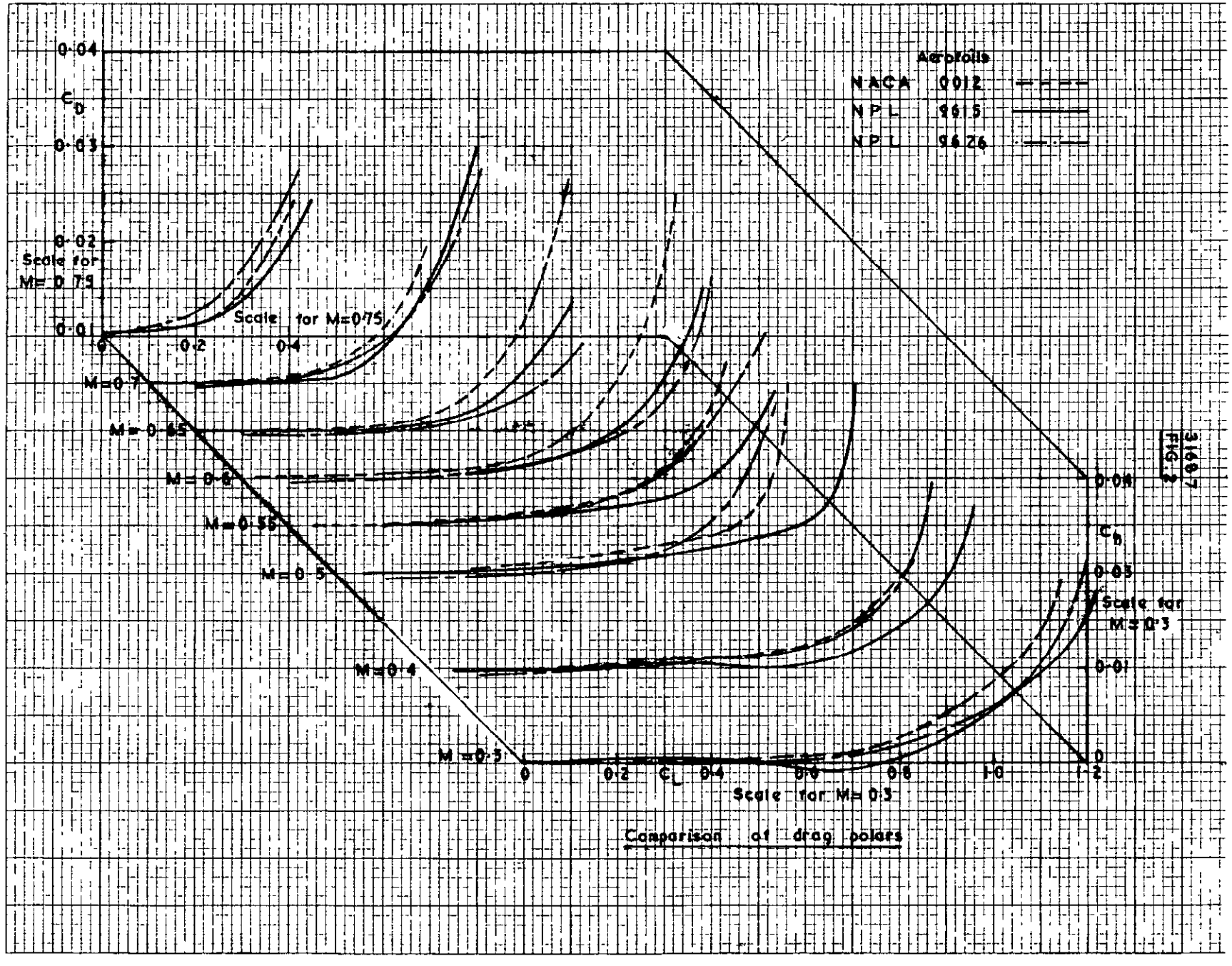
Aerofoils
NACA 0012
NPL 9615
NPL 9626
$C_D$
0·04
0·03
0·02
0·01
Scale for M=0·75
0
0·2
0·4
M=0·7
M=0·65
M=0·6
M=0·55
M=0·5
M=0·4
M=0·3
$C_L$
0·6
0·8
1·0
1·2
Scale for M=0·3
$C_b$
Scale for M=0·3
Comparison of drag polars
3167

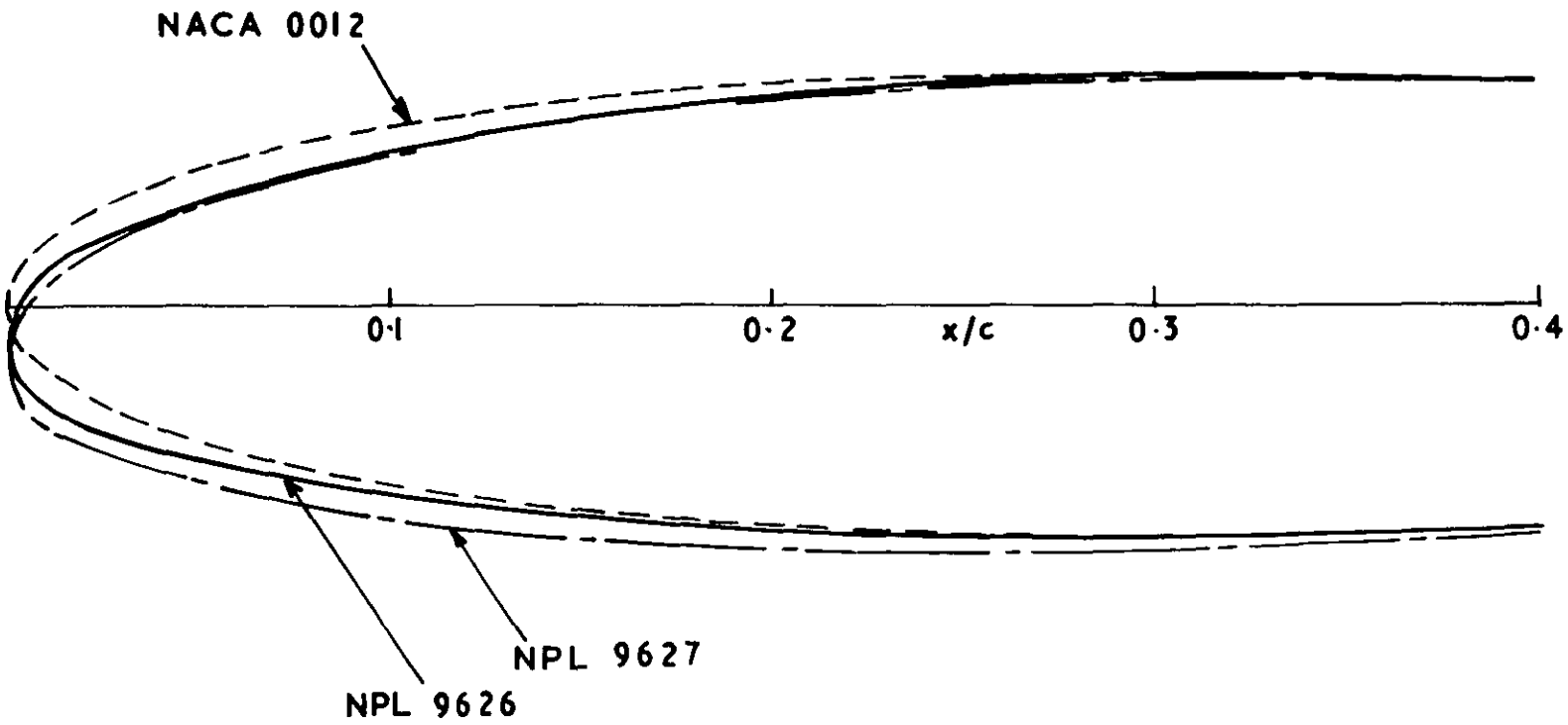


Aerofoil profiles

FIG. 3
31687

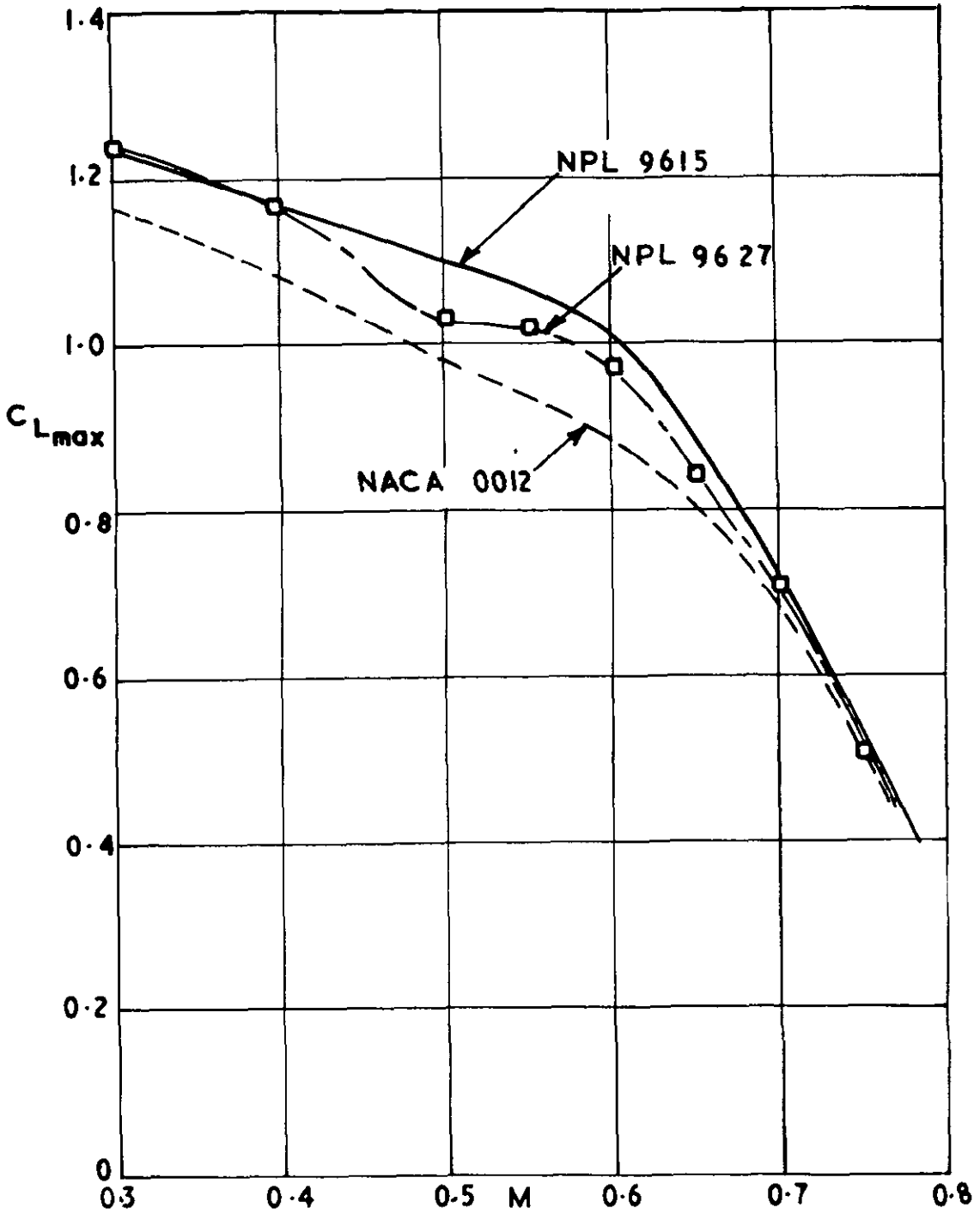


Variation of $C_{L\,max}$ with Mach number for NPL 9627

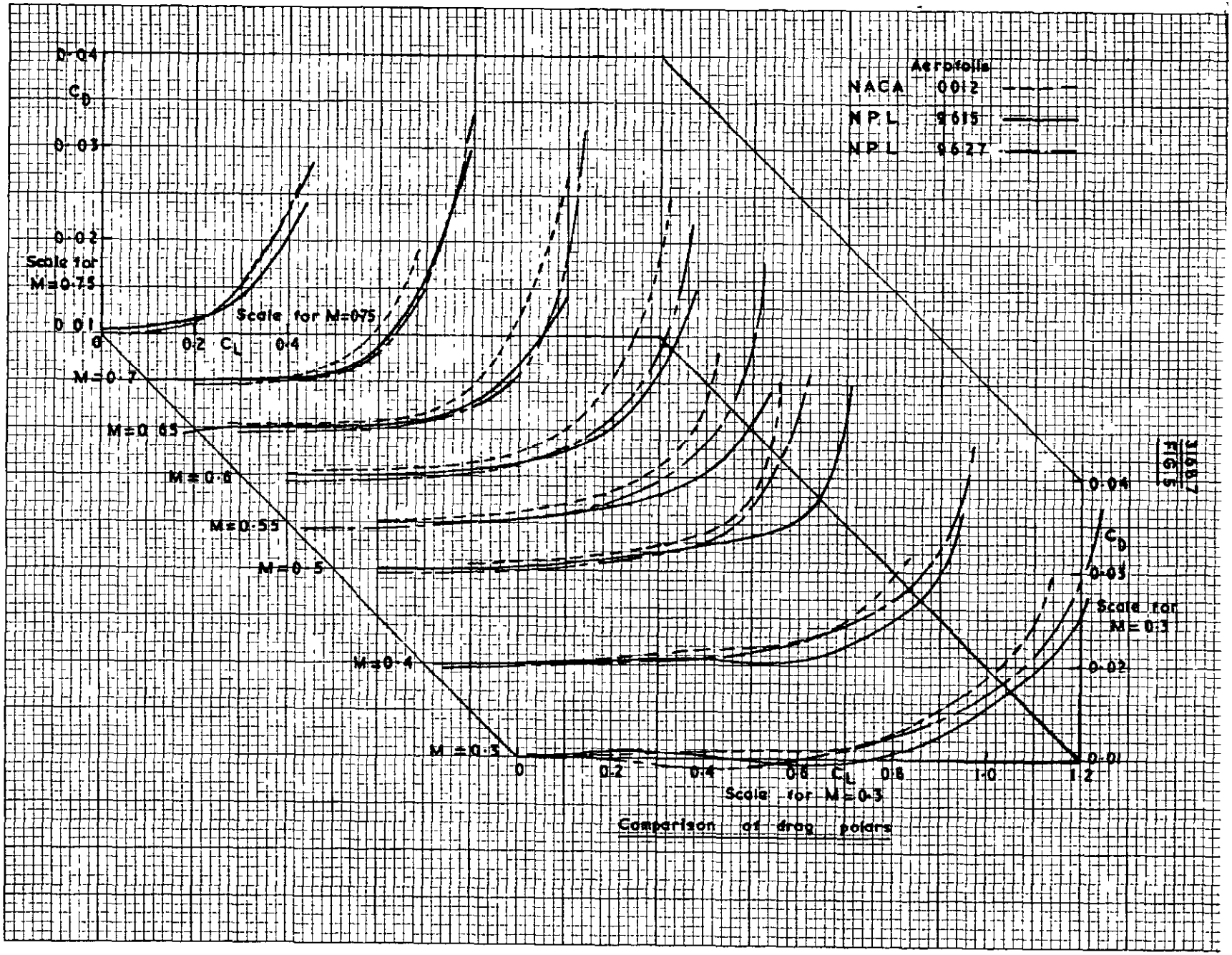
Aerofoils
NACA 0012
NPL 9615
NPL 9627
$C_D$
0·04
0·03
0·02
0·01
Scale for M=0·75
Scale for M=0·75
0
0·2
$C_L$
0·4
M=0·7
M=0·65
M=0·6
M=0·55
M=0·5
M=0·4
M=0·3
0·04
$C_D$
0·03
Scale for M=0·3
0·02
0·01
0
0·2
0·4
0·6
$C_L$
0·8
1·0
1·2
Scale for M=0·3
Comparison of drag polars

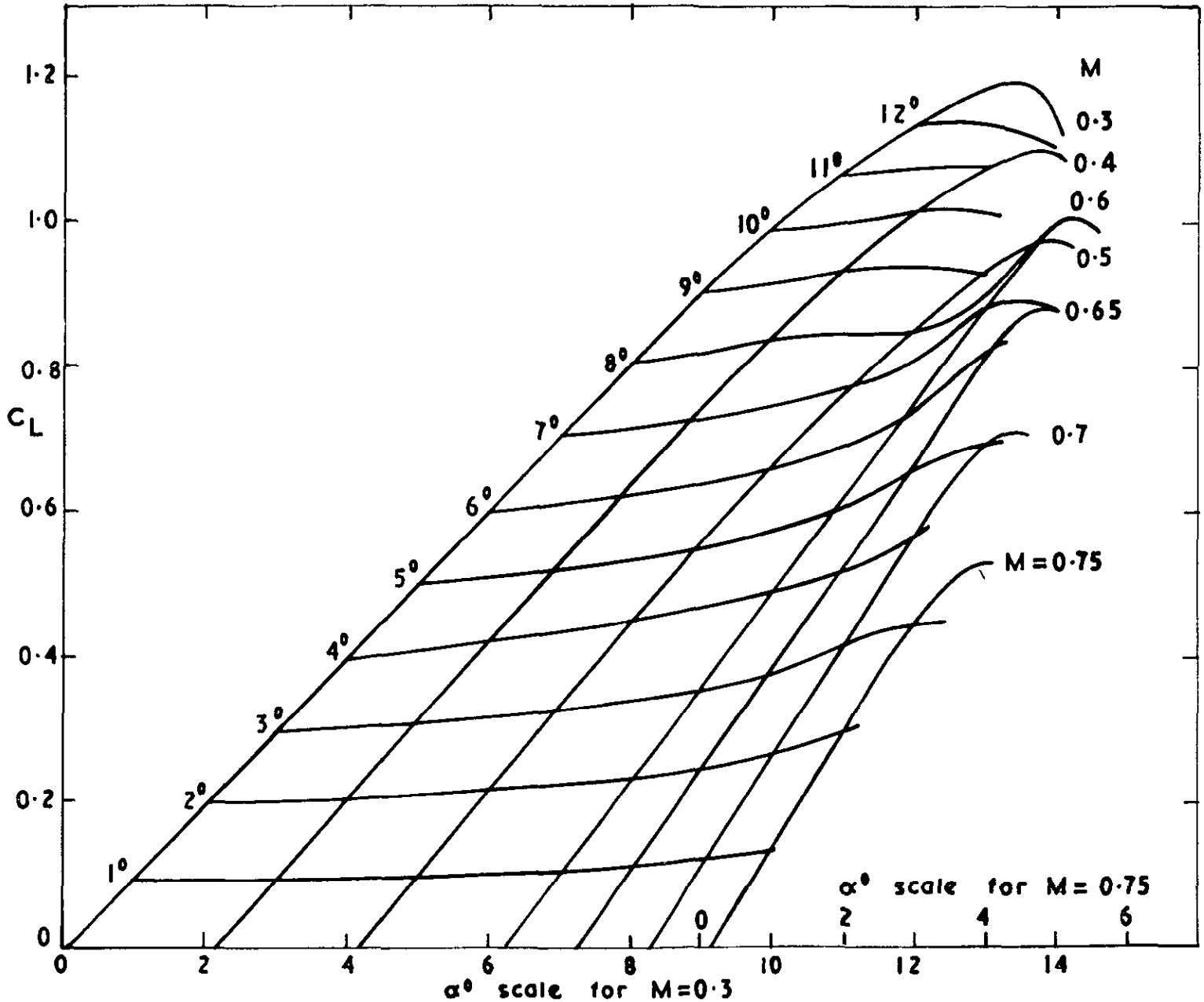


Variation of lift coefficient of NPL 9626 with incidence and Mach number

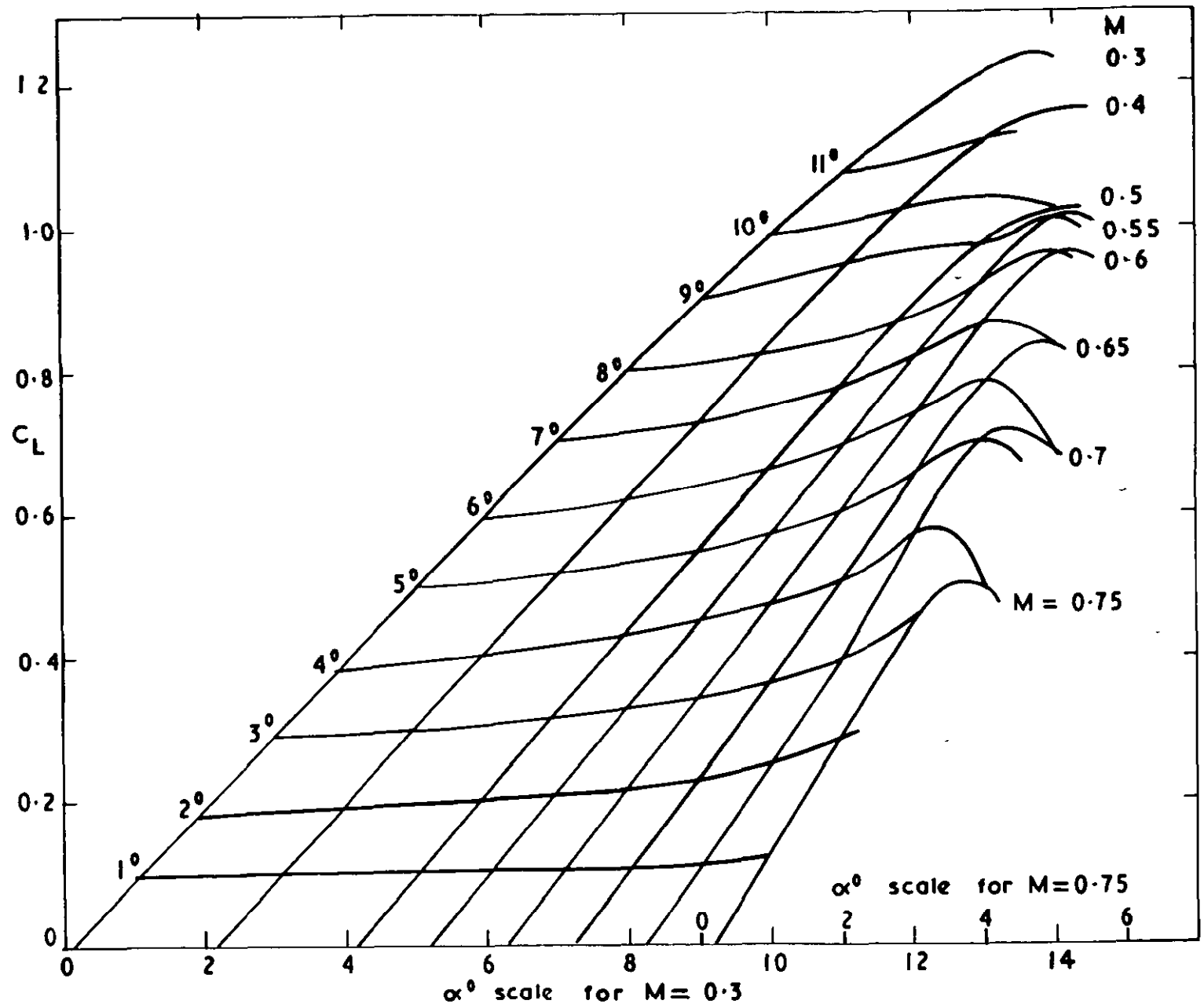


Variation of lift coefficient of NPL 9627 with incidence and Mach number

31687
FIG.7

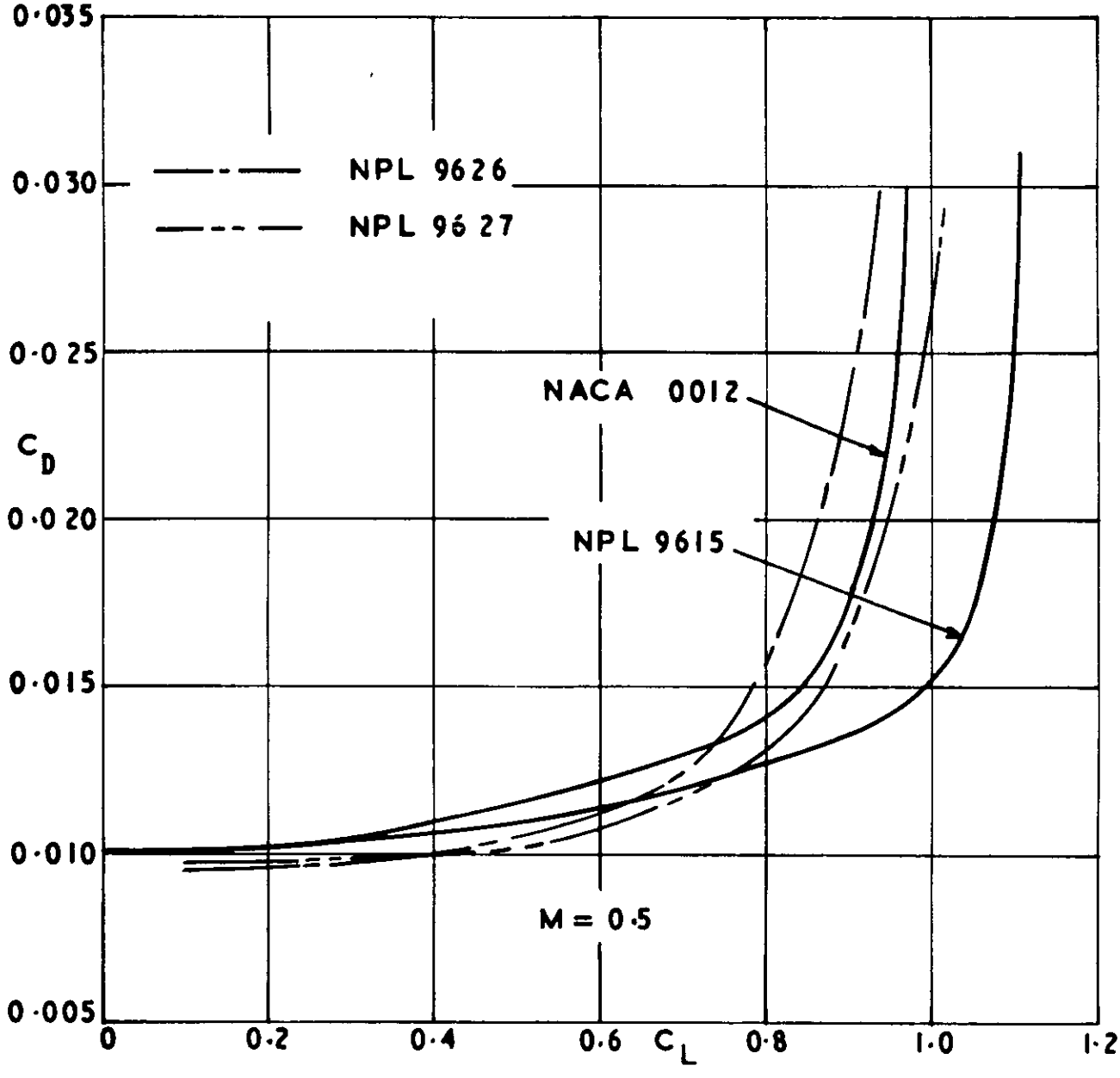


Comparison of variations of drag with lift at M = 0·5

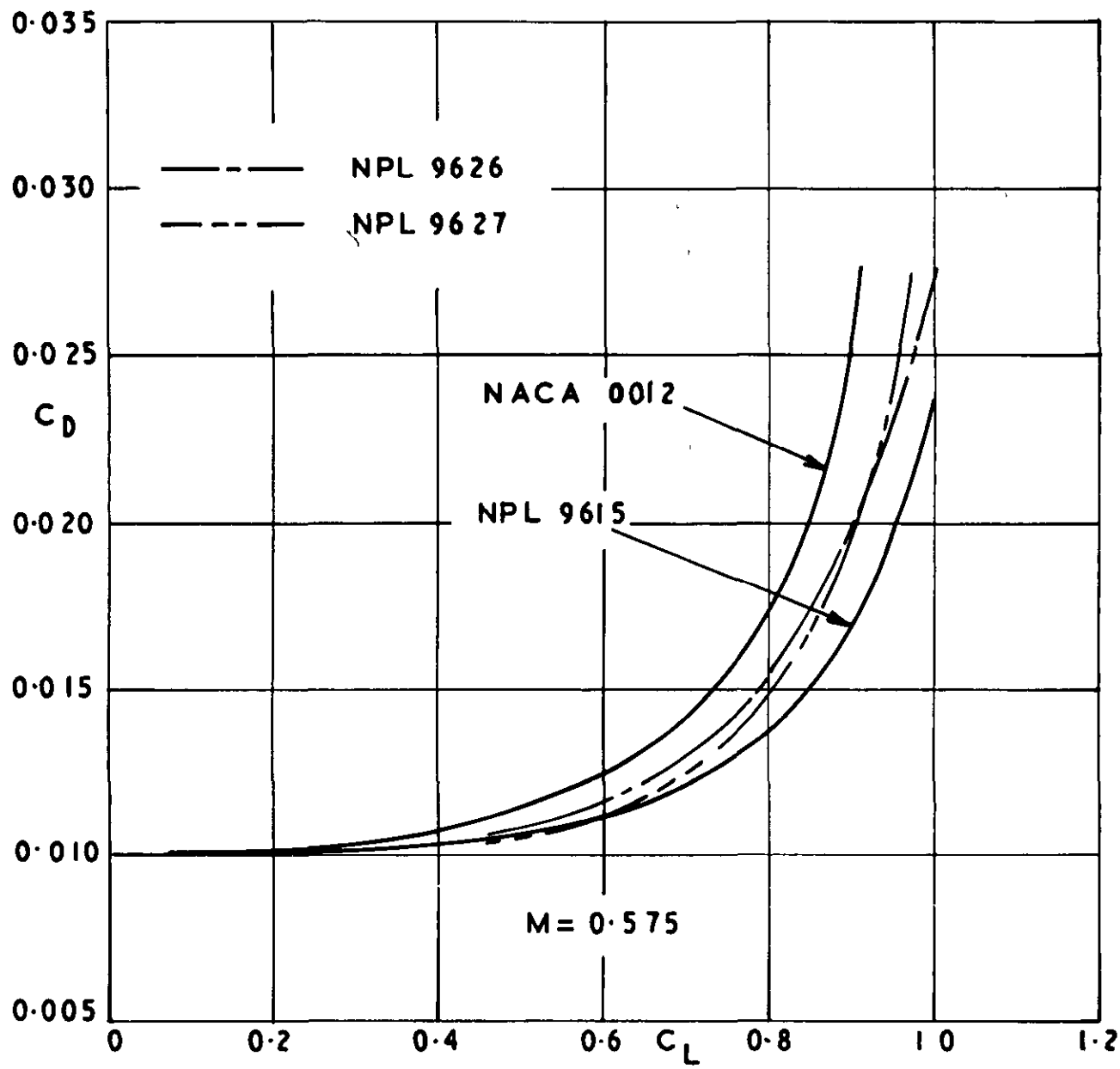


Comparison of variations of drag with lift at M = 0·575

31687
FIG. 10

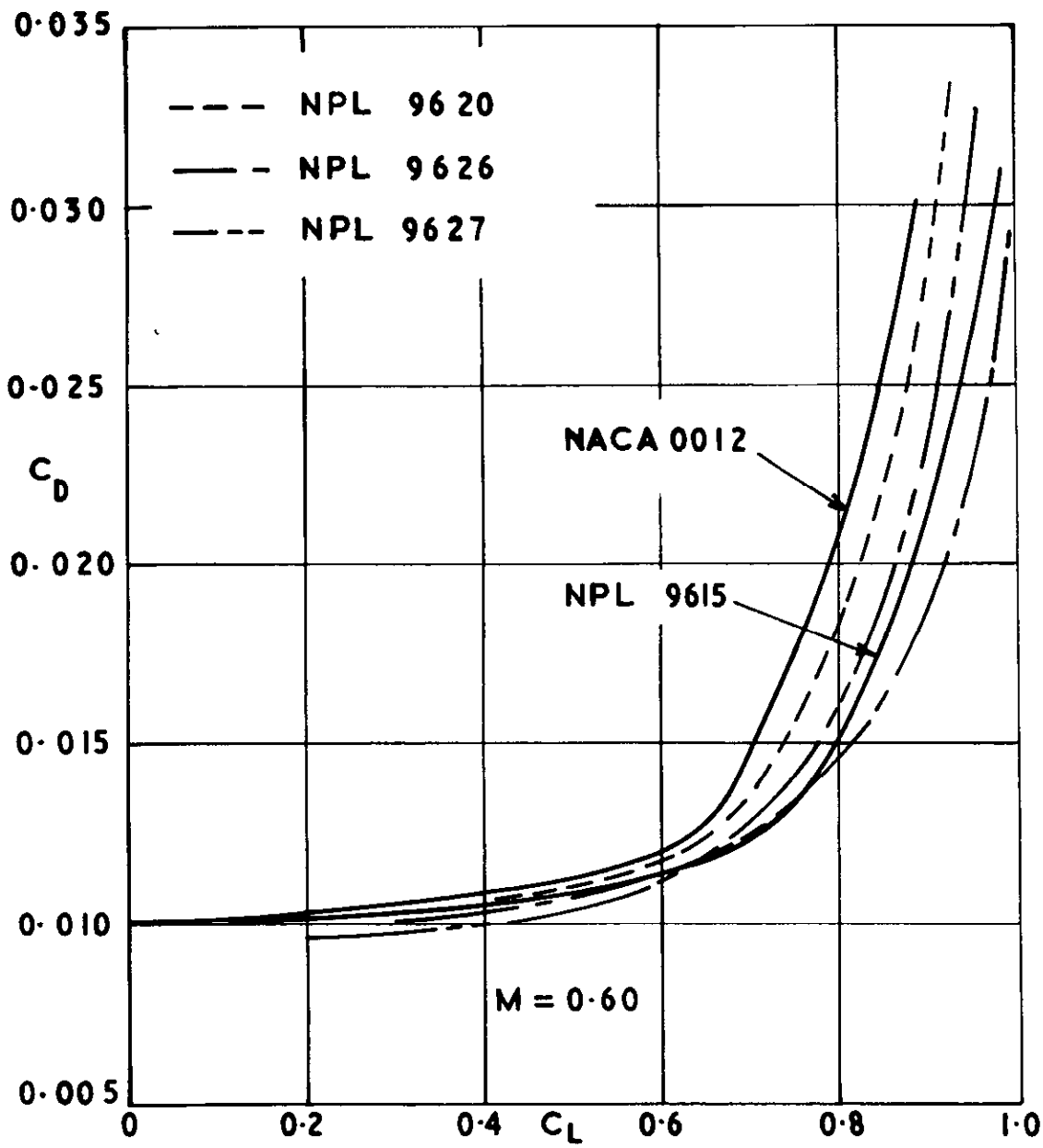


Comparison of variations of drag with lift at M = 0·6

31687
FIG. 11

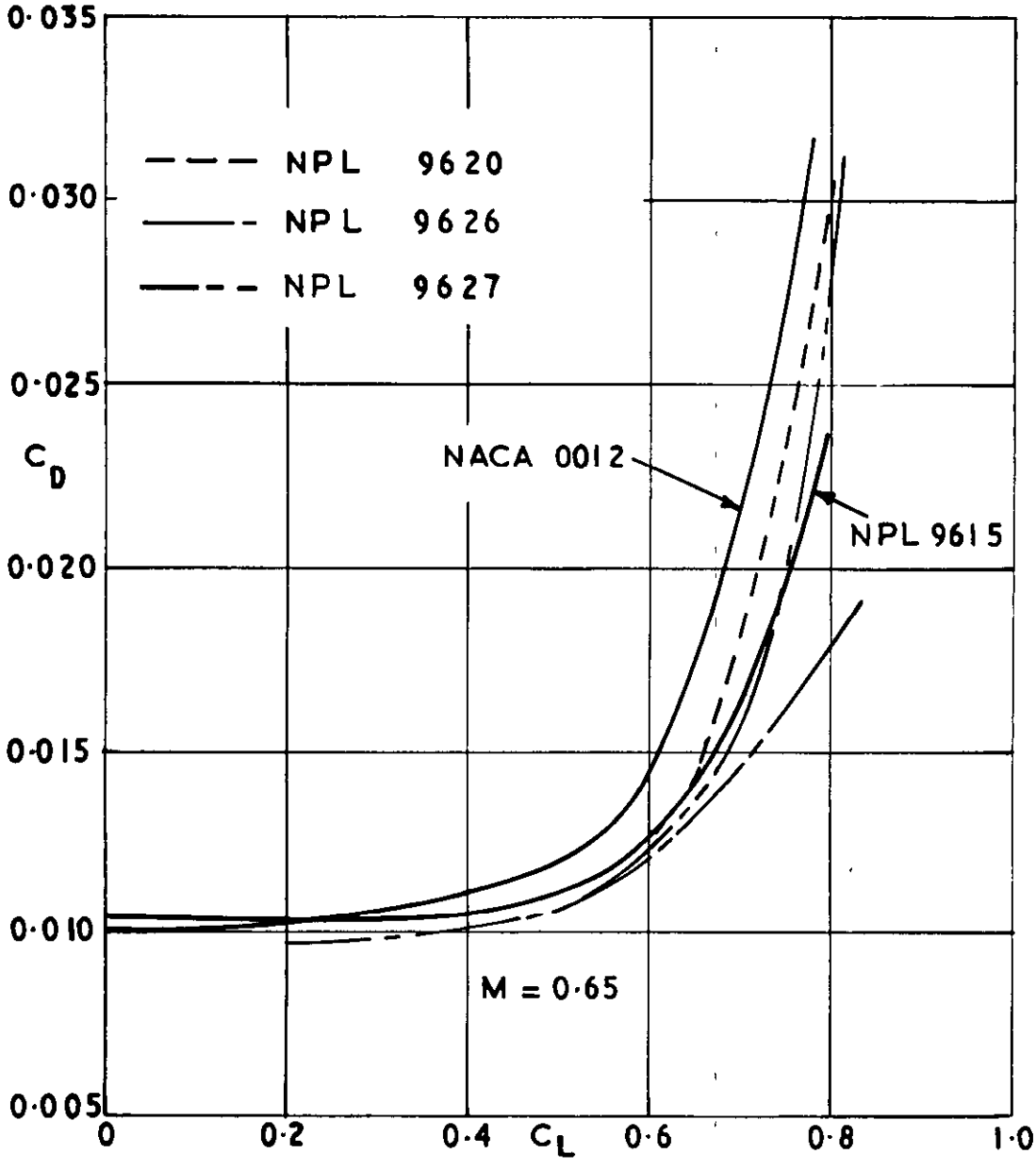


Comparison of variations of drag with lift at M = 0·65

31687
FIG.12

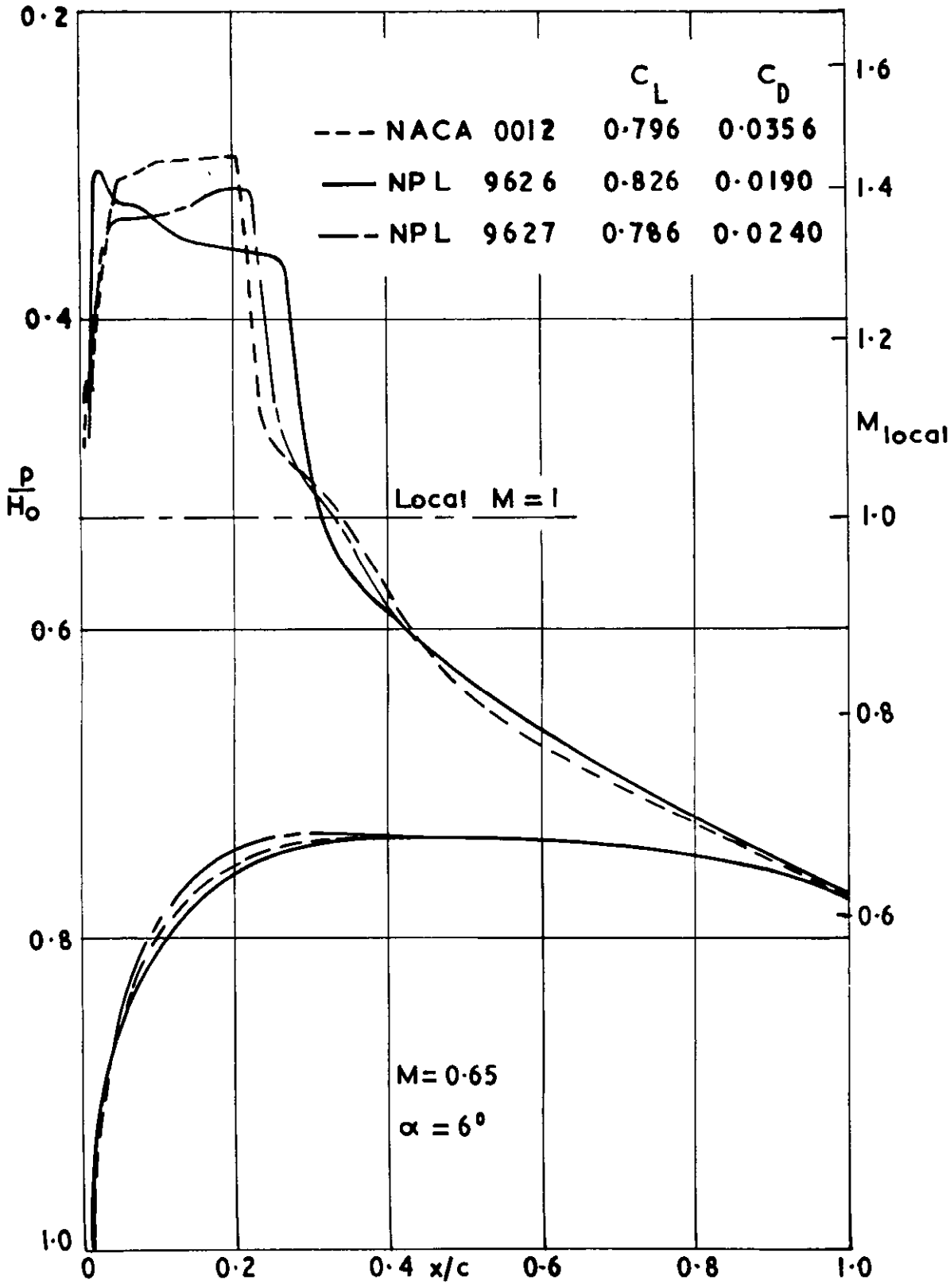


Experimental pressure distributions at M = 0·65

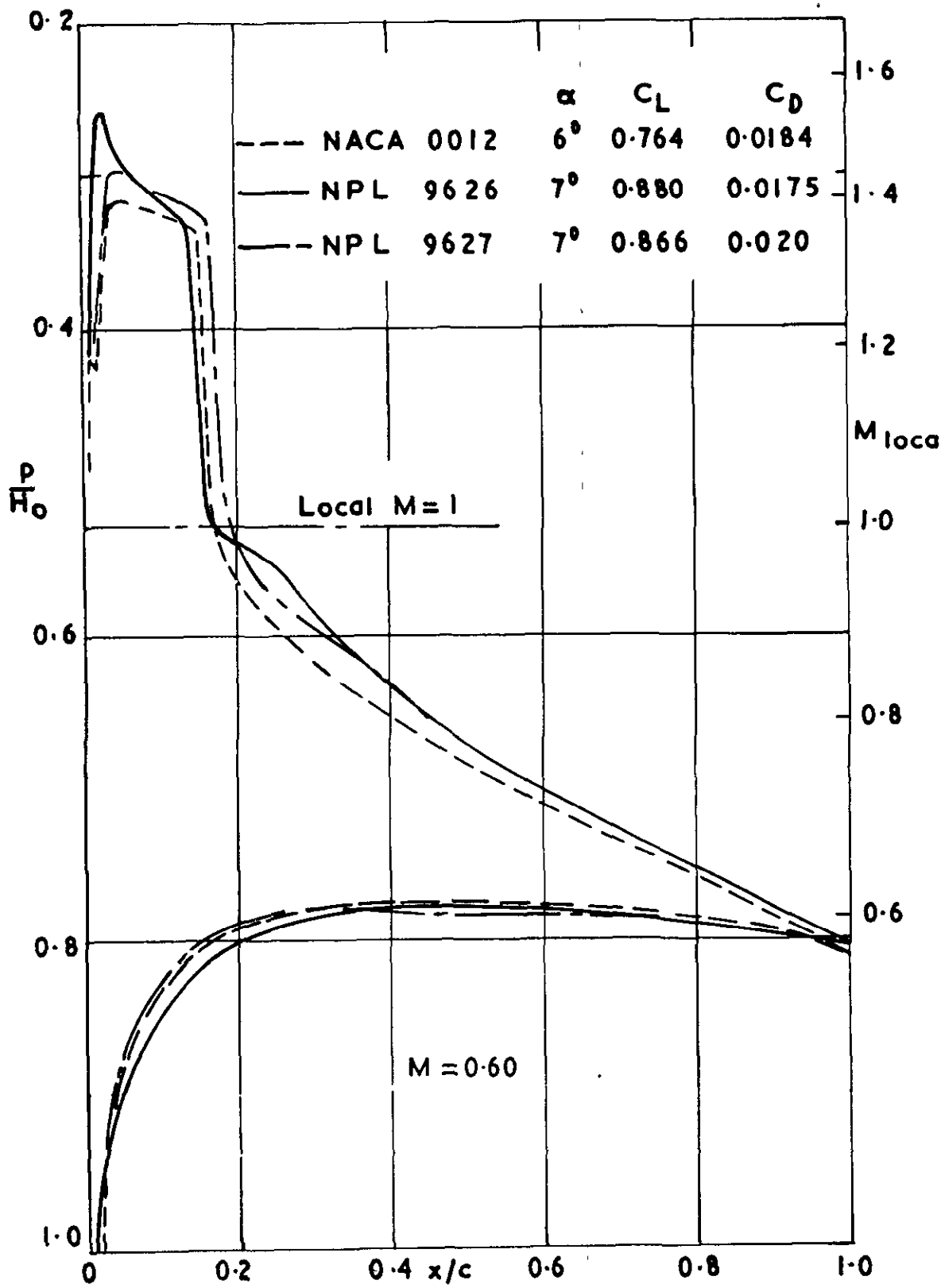


Experimental pressure distributions at M = 0·60

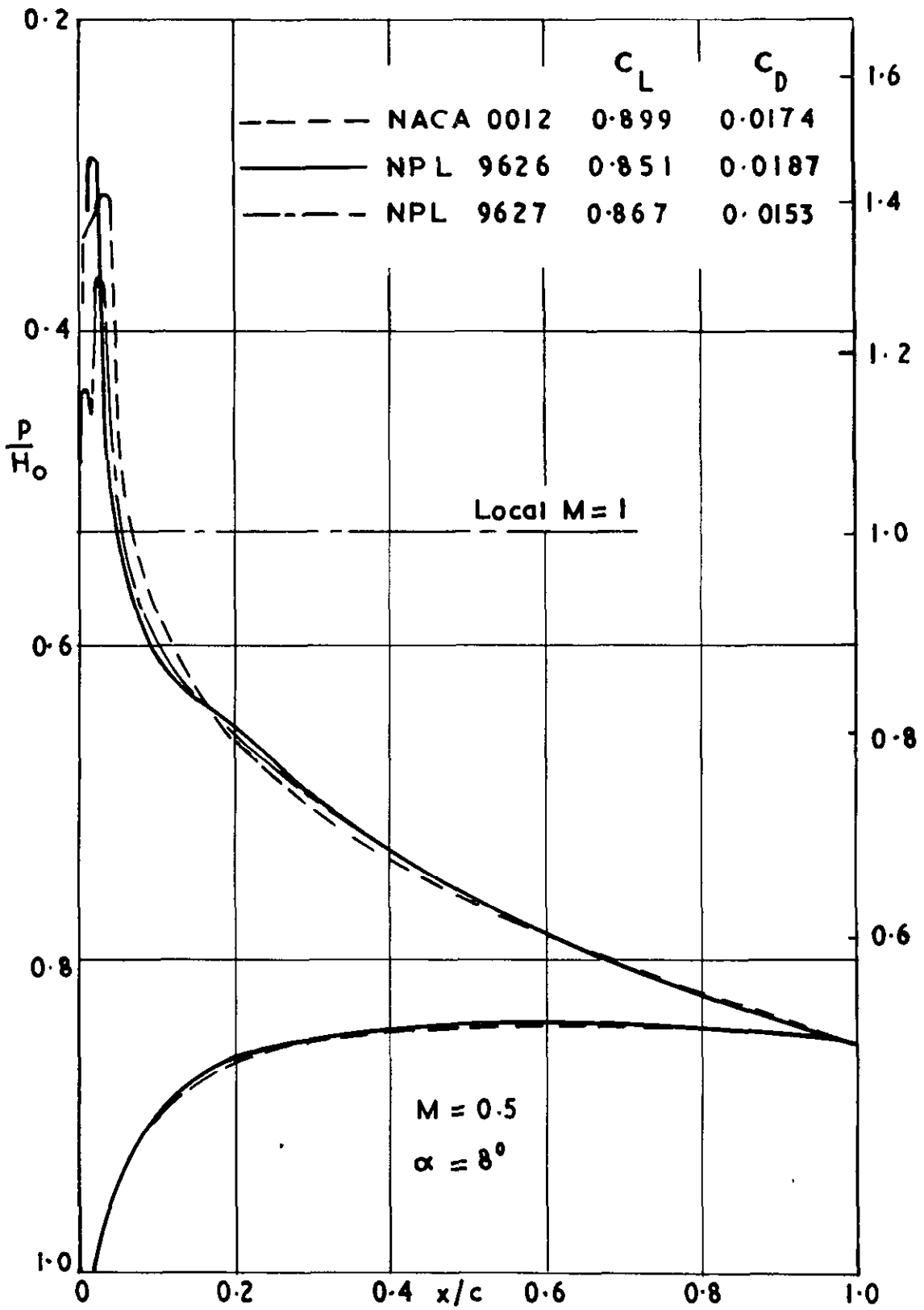


Experimental pressure distributions at M = 0·5

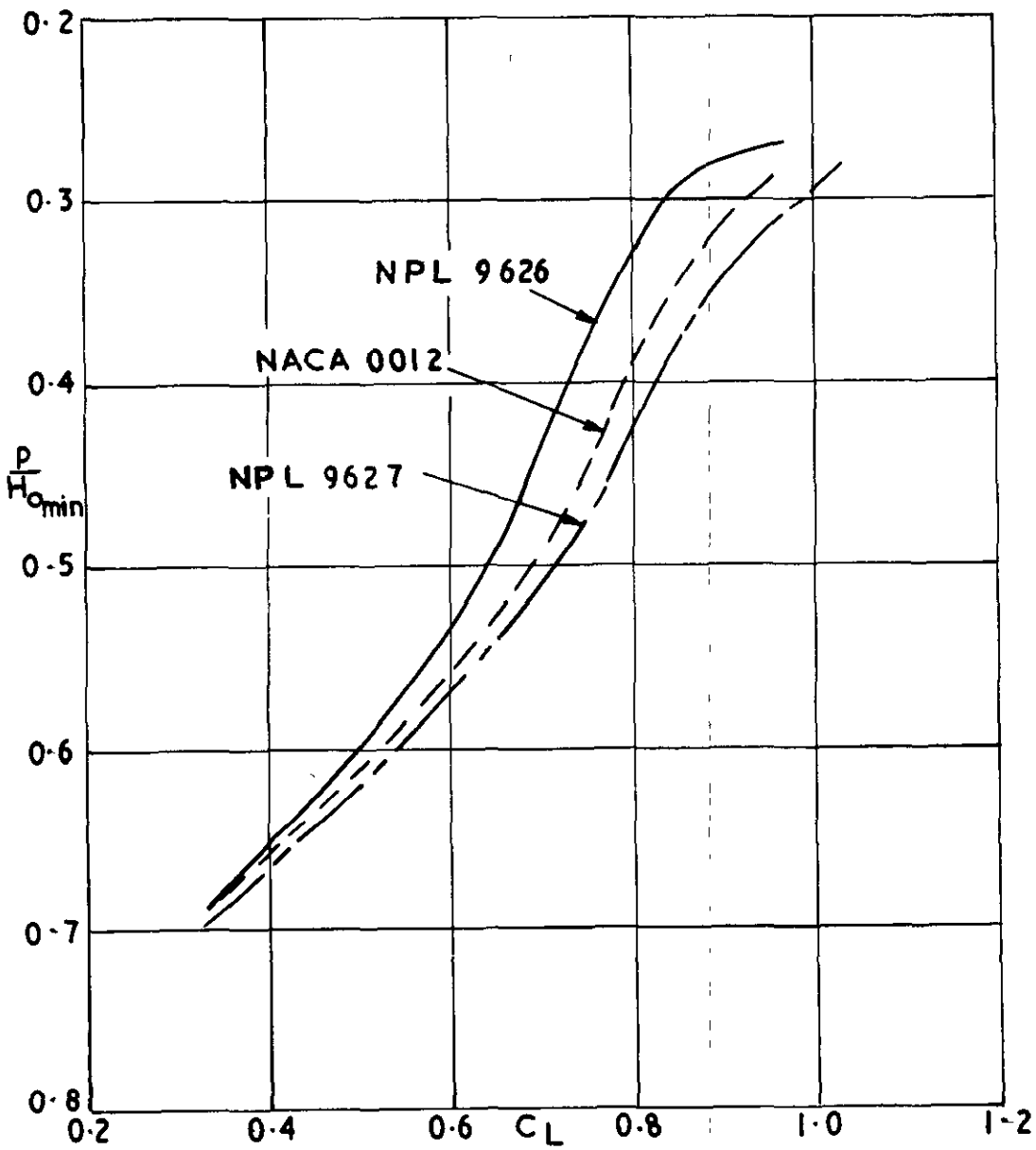


Measured variation of height of leading-edge peak with lift at M = 0·5

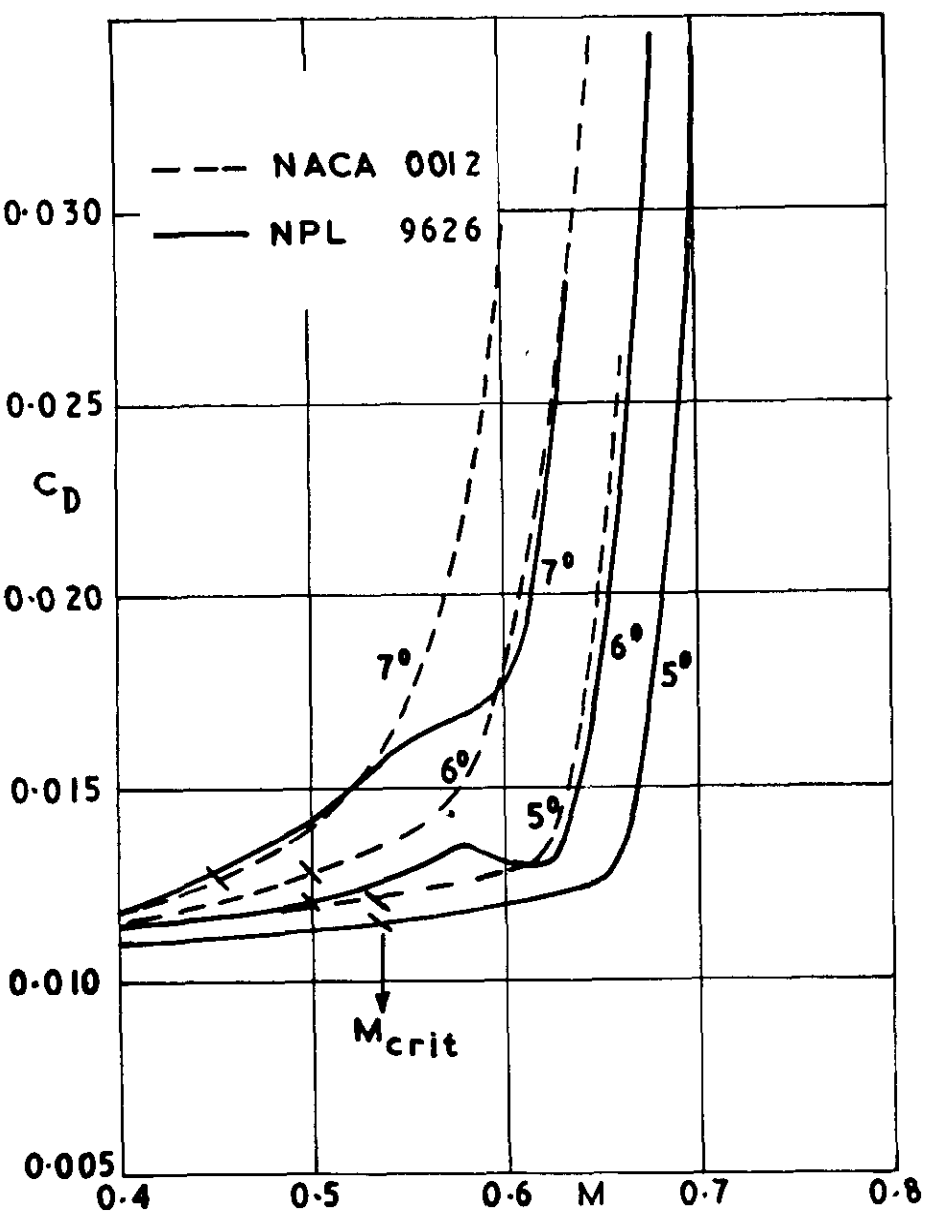


Variation of drag coefficient with Mach number for NPL 9626 and NACA 0012

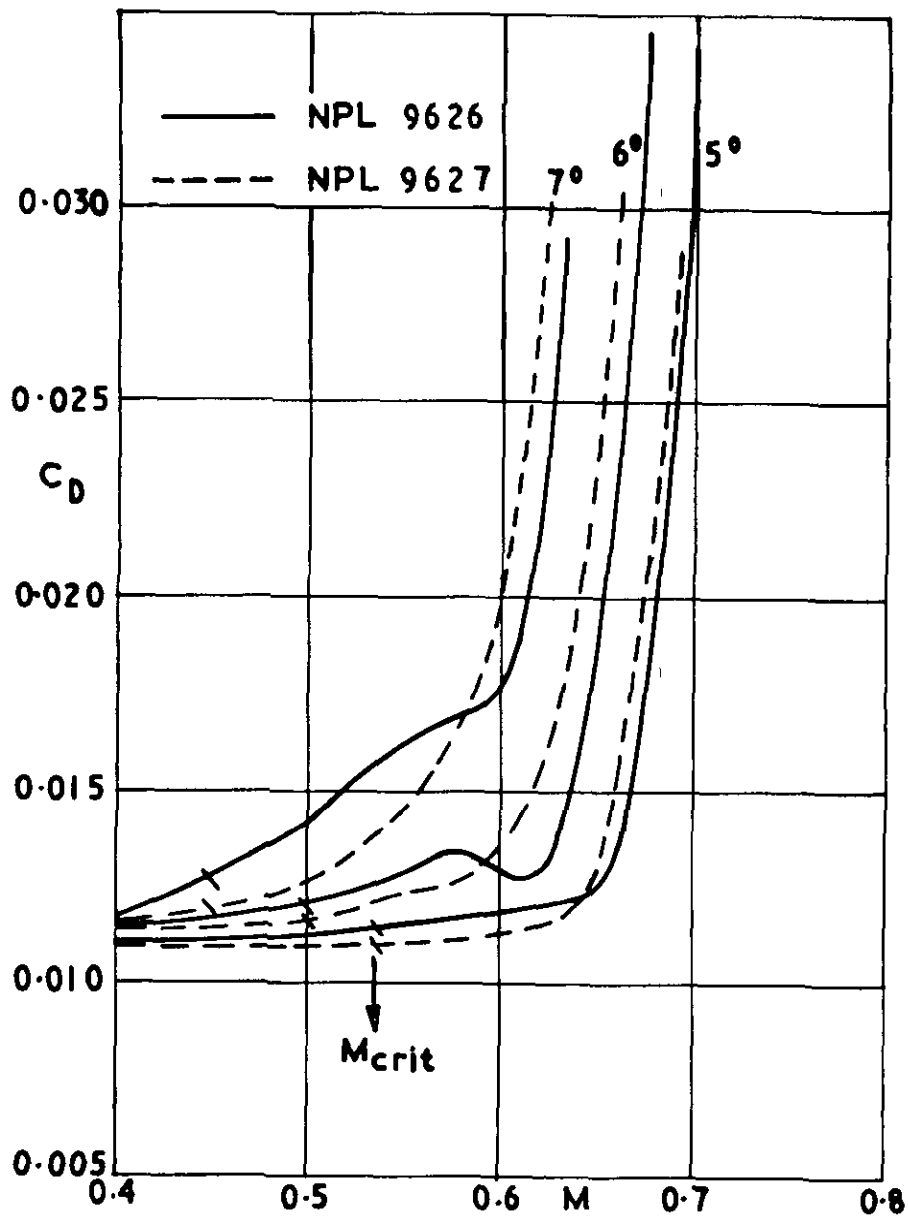


Variation of drag coefficient with Mach number for NPL 9626 and NPL 9627

31687
FIG 18

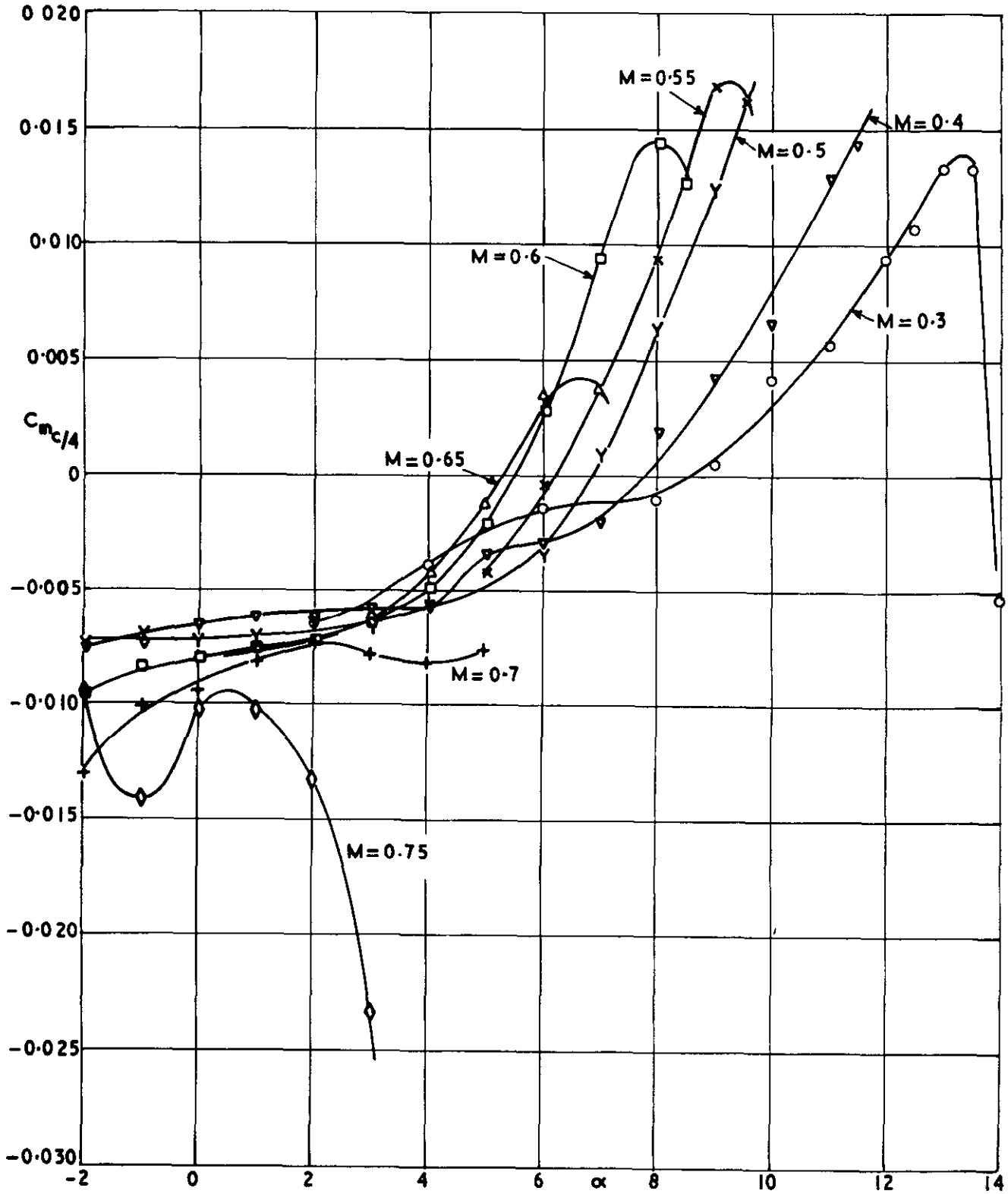


Variation of quarter-chord pitching moment with incidence and Mach number for NPL 9626

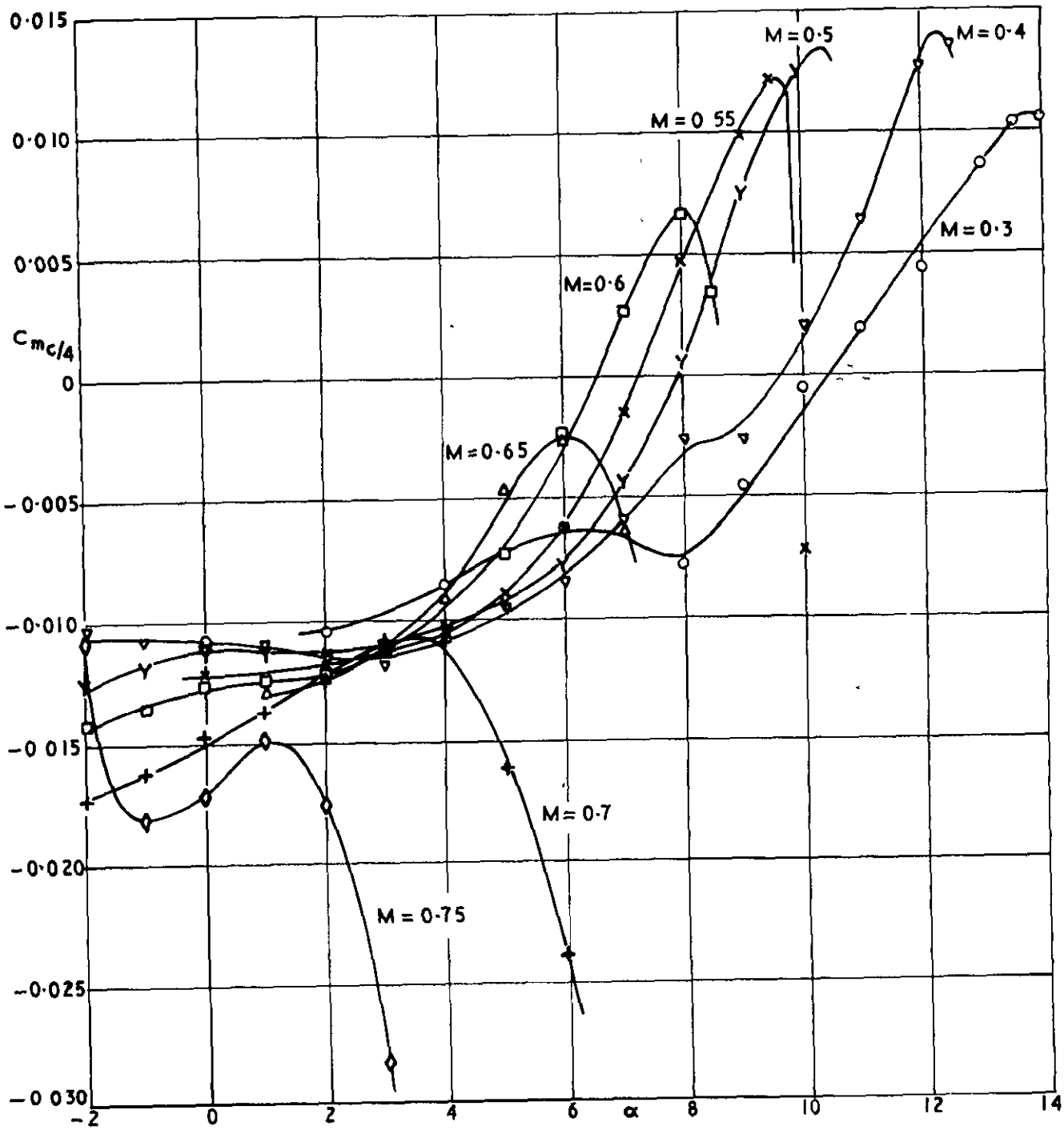


Variation of quarter-chord pitching moment with incidence and Mach number for NPL 9627

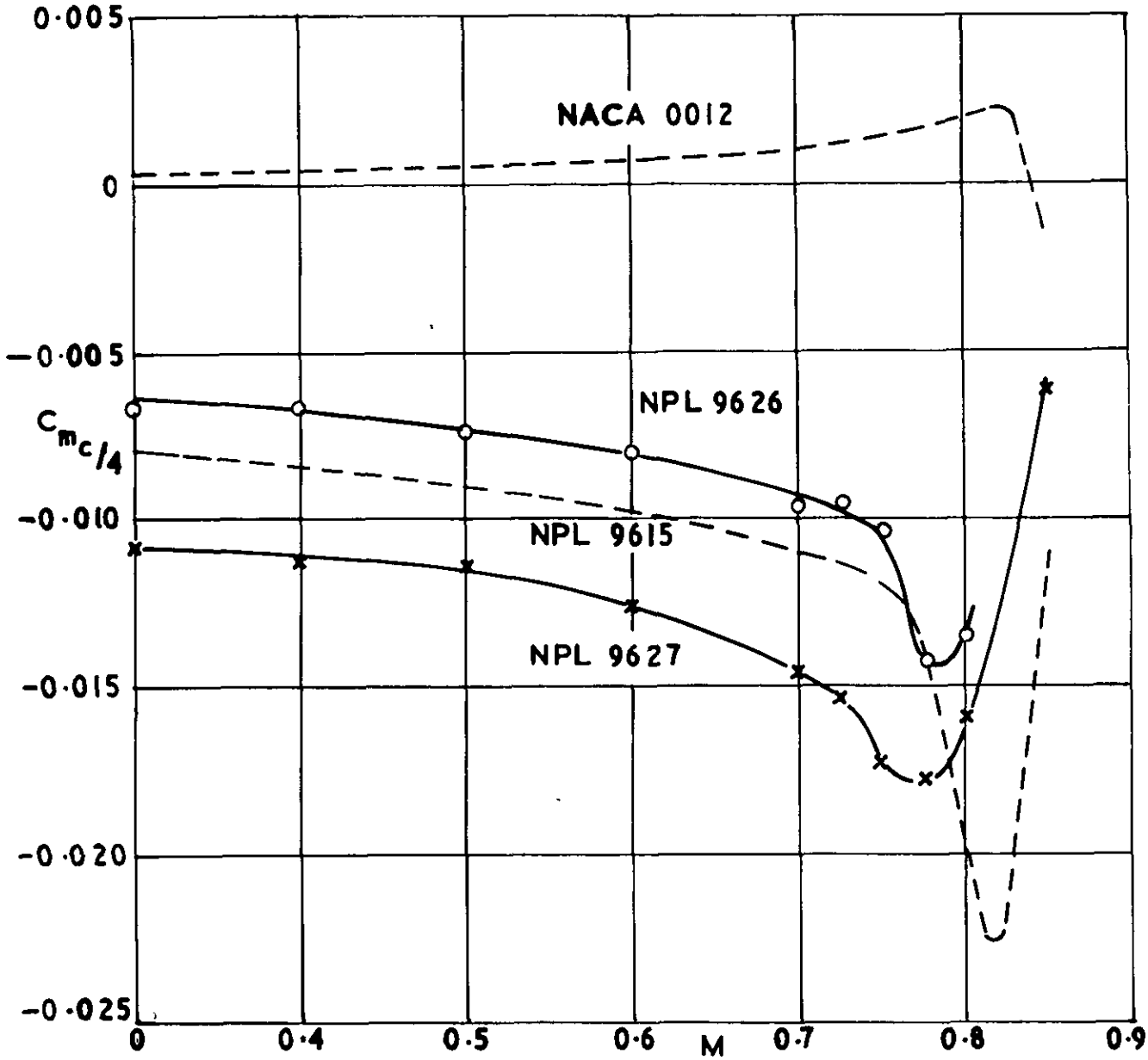


Comparison of variations of quarter-chord pitching moment with Mach number for near zero lift conditions

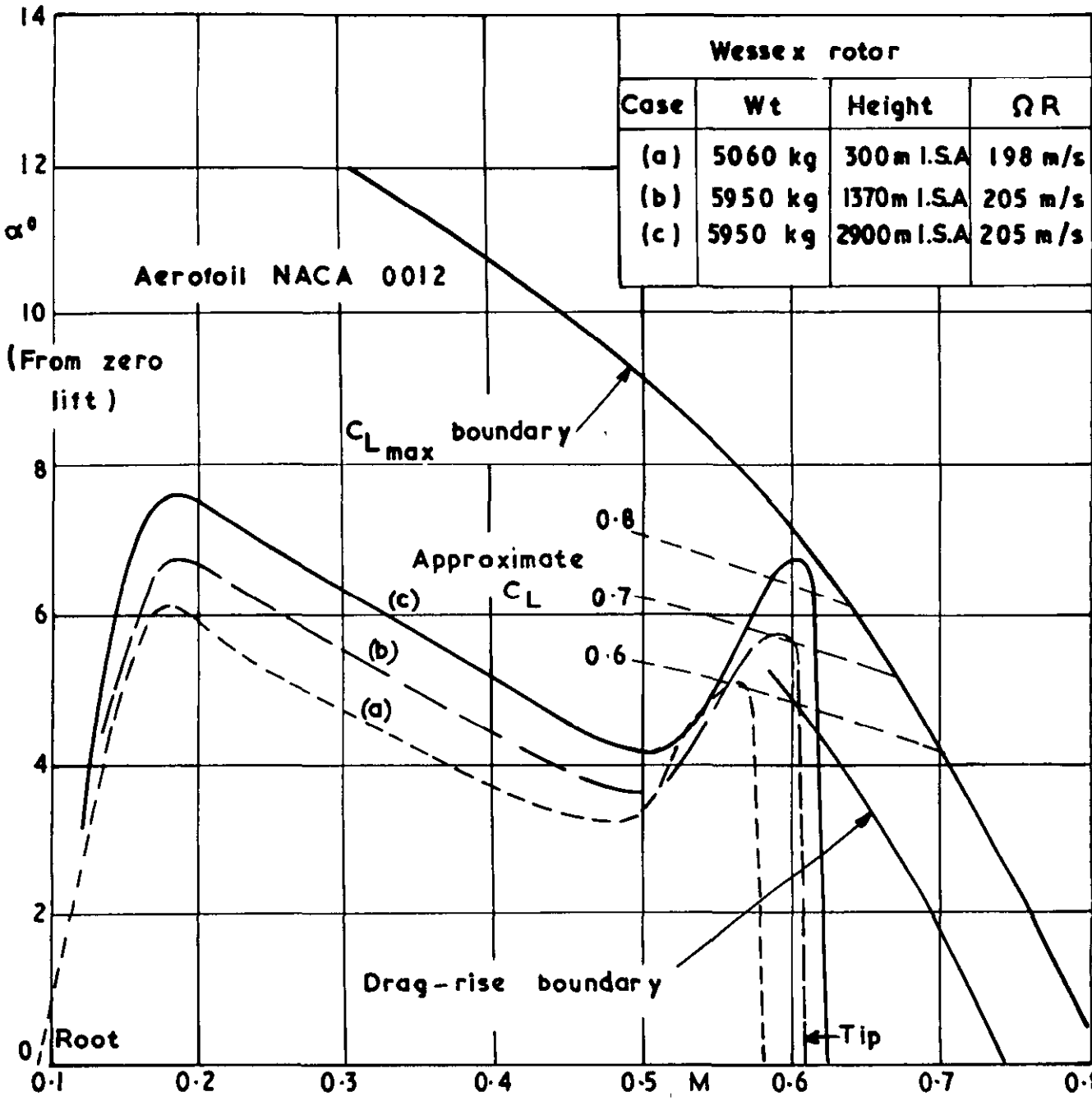


Wessex blade demands in hover

31687
FIGS. 22 & 23

FIG. 22

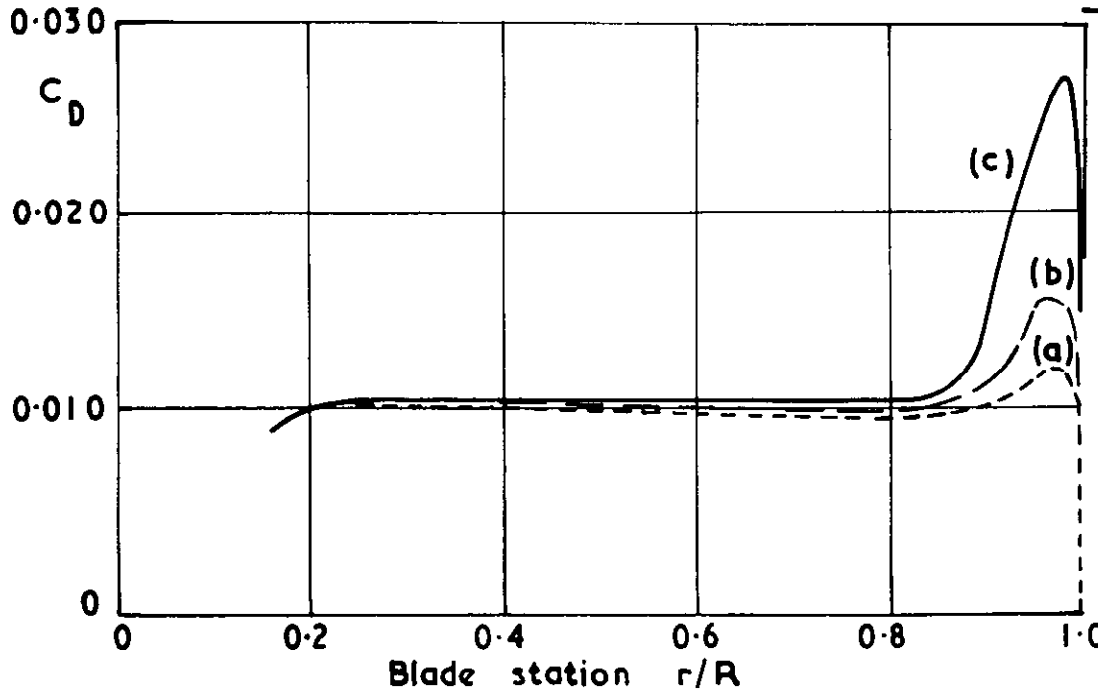


Radial distribution of blade drag. Cases as Fig. 21

FIG. 23

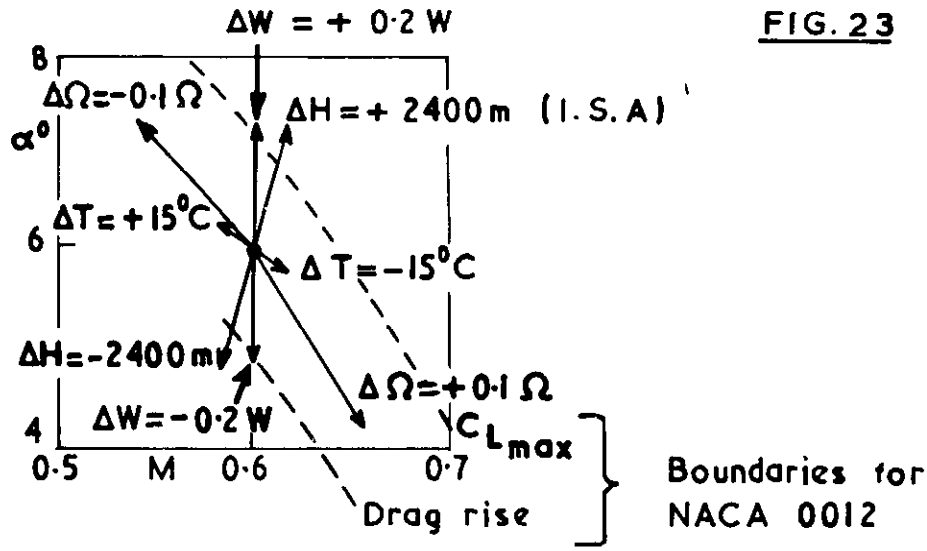


Diagram illustrating possible movements in peak demands for isolated changes in A.U.W., I.S.A. altitude, temperature and rotational speed

31687
FIG 24

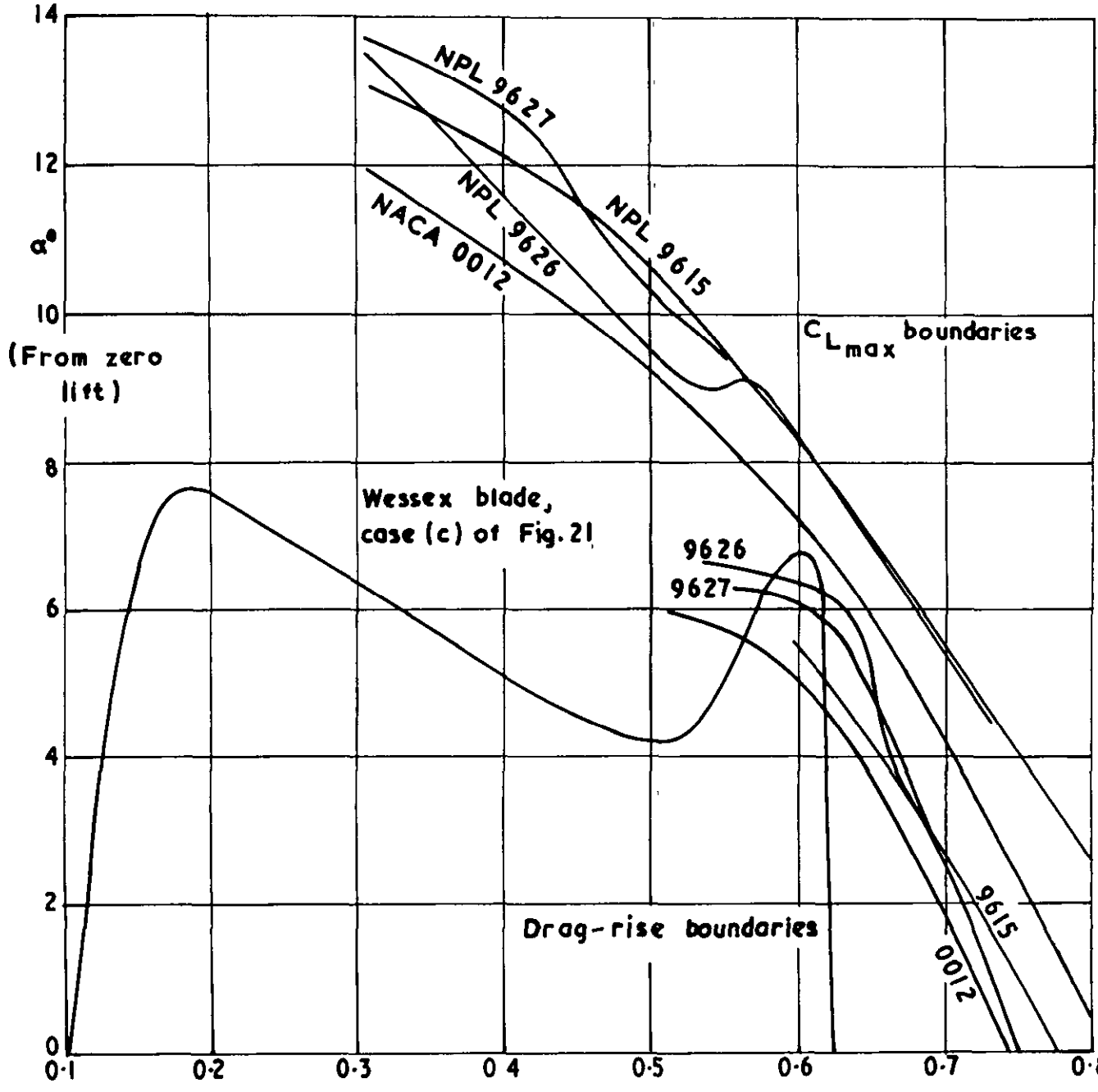


Comparison of drag rise boundaries and $C_{L_{max}}$ boundaries for various aerofoils

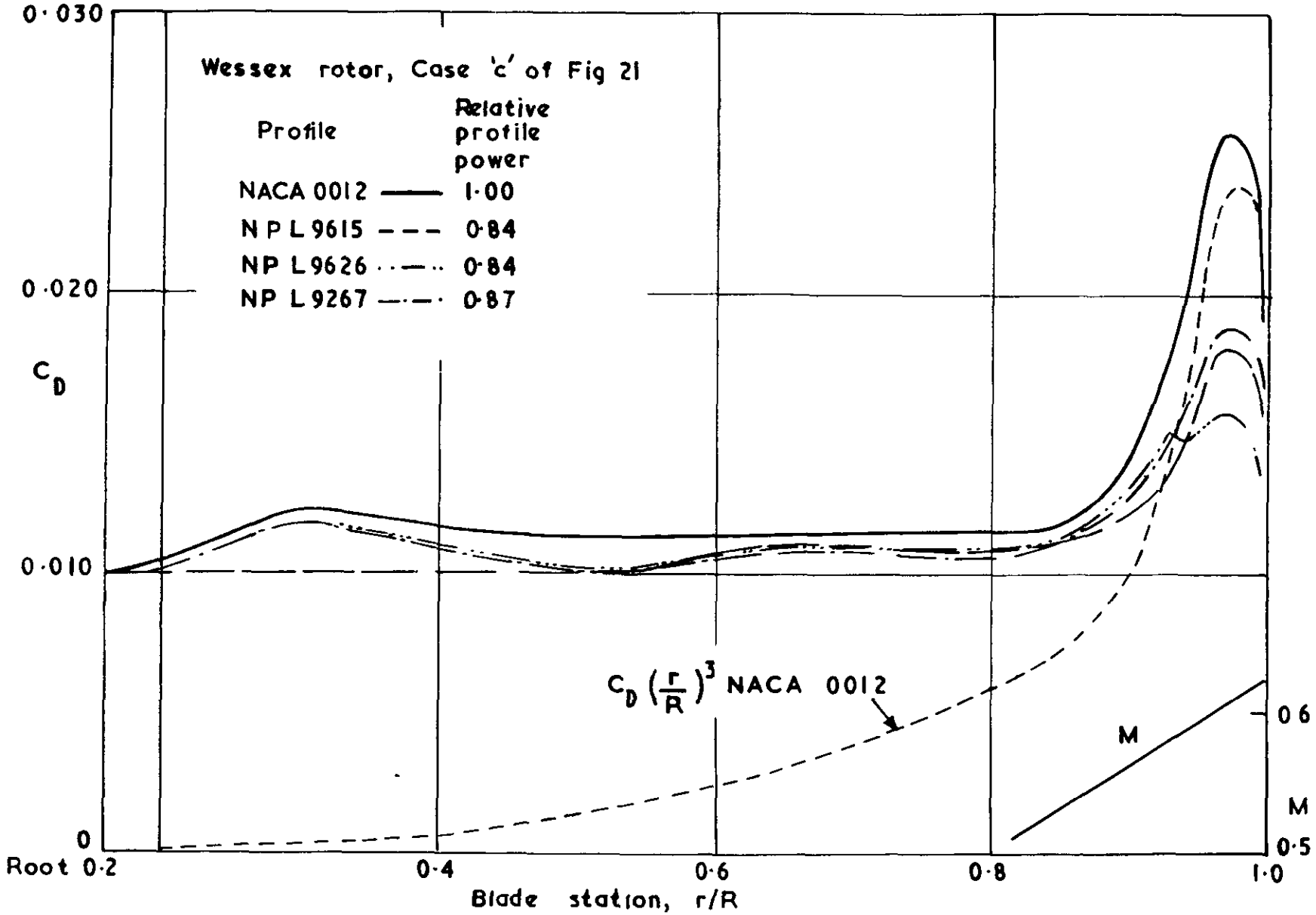


Effect of profile on Case ('c') radial distribution of blade drag

31687
FIG.25

31687
FIG. 26

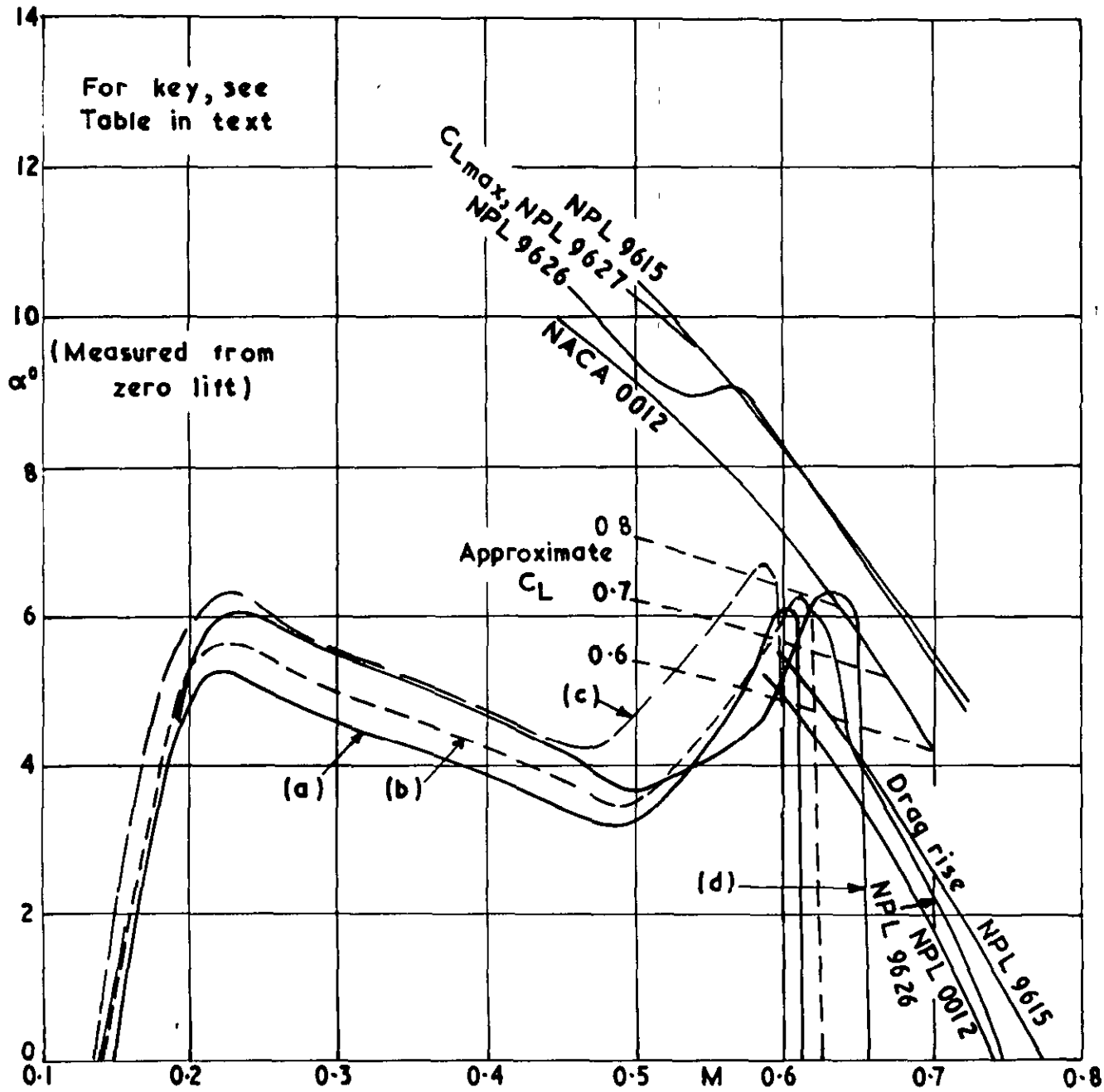


SUD 330 blade demands in hover

31687
FIG.27

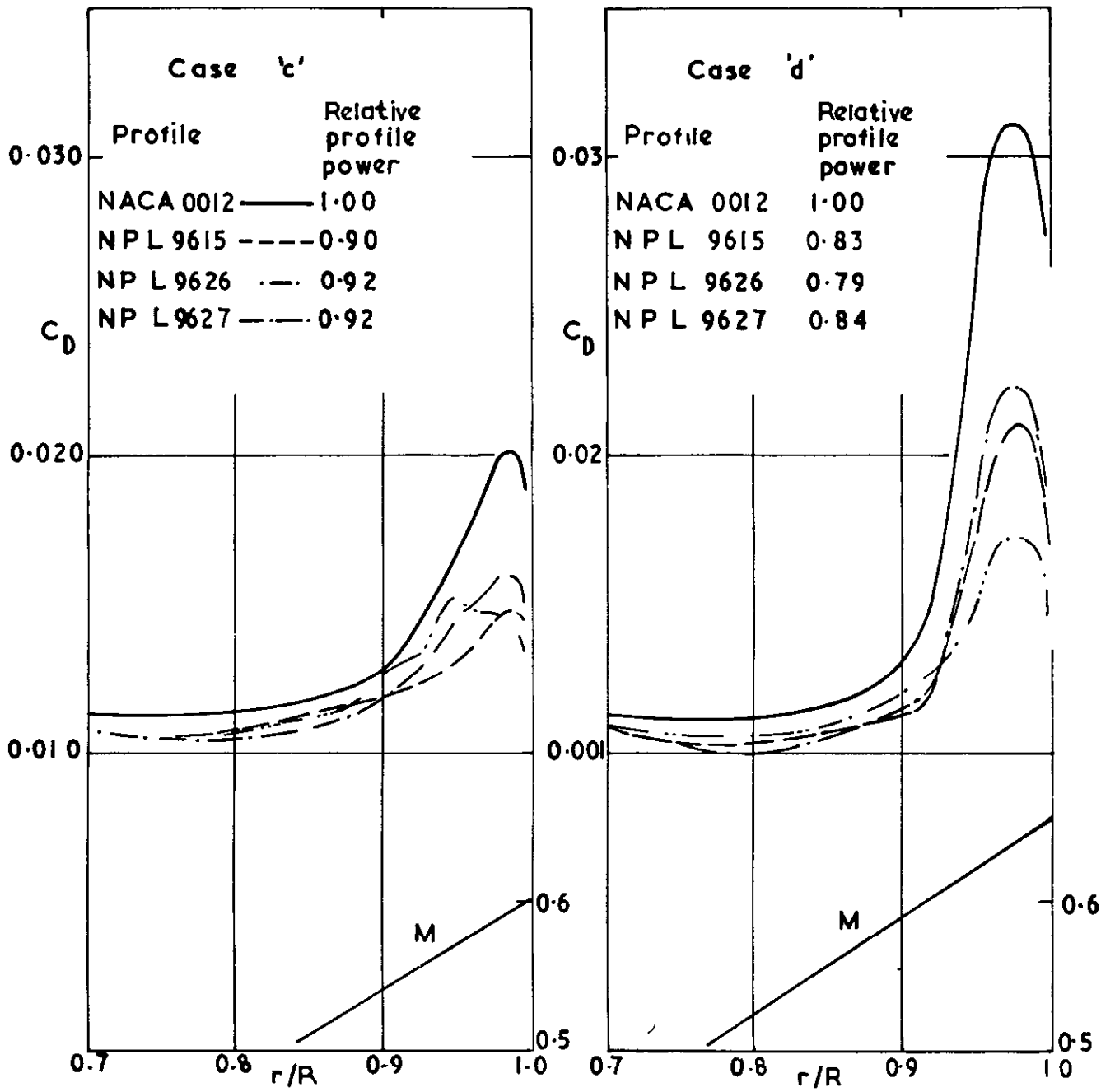


Case 'c' Weight 6480 kg, 1525 m, I.S.A. + 20° C
Case 'd' Weight 6160 kg, 3350 m, I.S.A. – 20° C

Effect of profile on radial distribution of blade drag on SUD 330 rotor

ARC CP No.1262
November, 1969
Wilby, P. G., Gregory, N. and Quincey, V. G.

AERODYNAMIC CHARACTERISTICS OF NPL 9626 AND NPL 9627 - FURTHER AEROFOILS DESIGNED FOR HELICOPTER ROTOR USE

Aerodynamic characteristics and ordinates are given for two modifications to the NACA 0012 profile with leading-edge camber that have been designed to produce reductions in wave drag in transonic flow. Analyses of hovering helicopter performance are given, to indicate the improvements that would follow from the adoption of either of these new aerofoils.

ARC CP No.1262
November, 1969
Wilby, P. G., Gregory, N. and Quincey, V. G.

AERODYNAMIC CHARACTERISTICS OF NPL 9626 AND NPL 9627 - FURTHER AEROFOILS DESIGNED FOR HELICOPTER ROTOR USE

Aerodynamic characteristics and ordinates are given for two modifications to the NACA 0012 profile with leading-edge camber that have been designed to produce reductions in wave drag in transonic flow. Analyses of hovering helicopter performance are given, to indicate the improvements that would follow from the adoption of either of these new aerofoils.

ARC CP No.1262
November, 1969
Wilby, P. G., Gregory, N. and Quincey, V. G.

AERODYNAMIC CHARACTERISTICS OF NPL 9626 AND NPL 9627 - FURTHER AEROFOILS DESIGNED FOR HELICOPTER ROTOR USE

Aerodynamic characteristics and ordinates are given for two modifications to the NACA 0012 profile with leading-edge camber that have been designed to produce reductions in wave drag in transonic flow. Analyses of hovering helicopter performance are given, to indicate the improvements that would follow from the adoption of either of these new aerofoils.

HER MAJESTY'S STATIONERY OFFICE

*Government Bookshops*

49 High Holborn, London WC1V 6HB
13a Castle Street, Edinburgh EH2 3AR
109 St Mary Street, Cardiff CF1 1JW
Brazennose Street, Manchester M60 8AS
50 Fairfax Street, Bristol BS1 3DE
258 Broad Street, Birmingham B1 2HE
80 Chichester Street, Belfast BT1 4JY

*Government publications are also available through booksellers*

C.P. No. 1262

ISBN 0 11 470820 7